

AERO-ASTRONAUTICS REPORT NO. 244

352550

FINAL REPORT ON NASA GRANT NO. NAG-1-516,  
OPTIMIZATION AND GUIDANCE OF FLIGHT TRAJECTORIES  
IN THE PRESENCE OF WINDSHEAR, 1984-89

by

A. MIELE

*NAG-1-516*

(NASA-CR-186163) OPTIMIZATION AND GUIDANCE  
OF FLIGHT TRAJECTORIES IN THE PRESENCE OF  
WINDSHEAR Final Report, 1984 - 1989 (Rice  
Univ.) 73 p CSDL 01C

N90-21747

Unclass  
0252550

G3/03

RICE UNIVERSITY

1989

AERO-ASTRONAUTICS REPORT NO. 244

FINAL REPORT ON NASA GRANT NO. NAG-1-516,  
OPTIMIZATION AND GUIDANCE OF FLIGHT TRAJECTORIES  
IN THE PRESENCE OF WINDSHEAR, 1984-89

by

A. MIELE

RICE UNIVERSITY

1989

Final Report on NASA Grant No. NAG-1-516,  
Optimization and Guidance of Flight Trajectories  
in the Presence of Windshear, 1984-89<sup>1</sup>

by

A. Miele<sup>2</sup>

---

<sup>1</sup>This research was supported by NASA Langley Research Center, Grant No. NAG-1-516, by Boeing Commercial Airplane Company, and by Air Line Pilots Association.

<sup>2</sup>Foyt Family Professor of Aerospace Sciences and Mathematical Sciences, Aero-Astronautics Group, Rice University, Houston, Texas.

Abstract. This paper summarizes the research on the optimization and guidance of flight trajectories in the presence of windshear, performed by the Aero-Astronautics Group of Rice University during the period 1984-89. This research refers to windshear recovery systems and covers two major areas of investigation: optimal trajectories for take-off, abort landing, and penetration landing; and guidance schemes for take-off, abort landing, and penetration landing.

Key Words. Flight mechanics, windshear problems, take-off, abort landing, penetration landing, optimal trajectories, optimal control, feedback control, guidance strategies, piloting strategies.

## 1. Introduction

Low-altitude windshear is a threat to the safety of aircraft in take-off and landing. Over the past 20 years, some 30 aircraft accidents have been attributed to windshear. The most notorious ones are the crash of Eastern Airlines Flight 066 at JFK International Airport (1975), the crash of PANAM Flight 759 at New Orleans International Airport (1982), and the crash of Delta Airlines Flight 191 at Dallas-Fort Worth International Airport (1985). These crashes involved the loss of some 400 people and an insurance settlement in excess of 500 million dollars.

To offset the windshear threat, there are two basic systems: windshear avoidance systems and windshear recovery systems. A windshear avoidance system is designed to alert the pilot to the fact that a windshear encounter might take place; here, the intent is the avoidance of a microburst. A windshear recovery system is designed to guide the pilot in the course of a windshear encounter; here, the intent is to fly smartly across a microburst, if an inadvertent encounter takes place. Obviously, windshear avoidance systems and windshear recovery systems are not mutually exclusive, but complementary to one other.

Examples of windshear avoidance systems are: ground-based mechanical systems (anemometers), ground-based radar systems (Doppler radar), and airborne systems (radar or lidar). Examples of windshear recovery systems are: maximum angle of attack guidance, constant pitch guidance, acceleration guidance, and

gamma guidance. At this time, some of the above avoidance systems and recovery systems appear to be promising. Further research is both necessary and desirable in order to let the dust settle and prior to making large commitments of funds to one system or another. For previous research, see Refs. 1-117.

1.1. Rice University Research on Windshear. This report refers to windshear recovery systems and summarizes the research performed at Rice University during the period 1984-89 under the sponsorship of NASA Langley Research Center, Boeing Commercial Airplane Company, and Air Line Pilots Association. This research was initiated in 1983 at the suggestion of Captain W. W. Melvin of Delta Airlines and ALPA. Its objective was: to study three problem areas, namely, take-off, abort landing, and penetration landing; for each problem area, to determine optimal trajectories, namely, trajectories minimizing a suitable performance index; for each problem area, to develop guidance schemes approximating the optimal trajectories in real time.

While the above problem areas are quite different from one another, they are related by common mathematical grounds and common procedures. The optimization problems can be solved by means of a single algorithm, the sequential gradient-restoration algorithm, developed by the Aero-Astronautics Group of Rice University over the years 1970-85. From a comprehensive study of the optimal trajectories, the dominant properties of these trajectories can be found. Then, these dominant properties are employed to develop guidance laws that it is desirable to

approach in actual flight. Finally, these guidance laws are implemented via feedback control schemes in such a way that the guidance trajectories approximate the optimal trajectories.

1.2. Wind Model. Although no two windshear encounters are exactly alike, two basic phenomena are always present: shear and downdraft. Therefore, it is important that these essential characteristics be present in the wind model employed in optimization and guidance studies. In this report, the assumed wind model has the following properties: (a) there is a transition from a uniform headwind to a uniform tailwind, with nearly constant shear in the core of the downburst; (b) the downdraft achieves maximum negative value at the center of the downburst; (c) the downdraft vanishes on the ground,  $h = 0$ ; and (d) the wind velocity components nearly satisfy the continuity equation and the irrotationality condition in the core of the downburst.

In this model, the horizontal shear (hence, the horizontal wind component) is independent of the altitude; and the downdraft (the vertical wind component) increases linearly with the altitude. Therefore, the wind model has the form

$$W_x = \lambda A(x), \quad W_h = \lambda (h/h_*) B(x). \quad (1)$$

Here, the parameter  $\lambda = \Delta W_x / \Delta W_{x*}$  characterizes the intensity of the windshear/downdraft combination; the function  $A(x)$  represents the distribution of the horizontal wind versus the

horizontal distance; the function  $B(x)$  represents the distribution of the vertical wind versus the horizontal distance; and  $h_*$  is a reference altitude,  $h_* = 1000$  ft. Also,  $\Delta W_x$  is the horizontal wind velocity difference (maximum tailwind minus maximum headwind) and  $\Delta W_{x*} = 100$  fps is a reference value for  $\Delta W_x$ .

Decreasing values of  $\lambda$  (hence, decreasing values of  $\Delta W_x$ ) correspond to milder windshears; conversely, increasing values of  $\lambda$  (hence, increasing values of  $\Delta W_x$ ) correspond to more severe windshears. Therefore, by changing the value of  $\lambda$ , one can generate shear/downdraft combinations ranging from extremely mild to extremely severe.

Figure 1 shows the functions  $W_x(x)$  and  $W_h(x,h)$ , computed for  $\lambda = 1$ , corresponding to  $\Delta W_x = 100$  fps. For other values of  $\lambda$  (hence, for other values of  $\Delta W_x$ ), the ordinates in Fig. 1 must be scaled proportionally to  $\lambda$  (hence, proportionally to  $\Delta W_x$ ).

1.3. Outline. The take-off problem is discussed in Section 2; the abort landing problem is considered in Section 3; and the penetration landing problem is presented in Section 4. Future developments are discussed in Section 5. Two appendices contain the equations of motion (Section 6) and the nomenclature (Section 7). The paper ends with an extensive bibliography on the windshear problem; see Refs. 1-65 for research done at Rice University under the present grant, and see Refs. 66-117 for research done elsewhere.

2. Take-Off Problem (Refs. 49-52, 54, 56, 61-65)

2.1. Optimal Trajectories. Optimal take-off trajectories were studied with the aid of the sequential gradient-restoration algorithm for optimal control problems. Several performance indexes were considered; the most reliable one was found to be the deviation of the absolute path inclination from the nominal value. Because the deviation has a maximum value along the flight path, attention was focused on minimizing the peak deviation. The resulting optimization problem is a minimax problem or Chebyshev problem of optimal control, in which the desired minimum performance index has the form

$$I_* = \min_{\alpha} I, \quad (2a)$$

$$I = \max_t |\gamma_e - \gamma_{e0}|, \quad 0 \leq t \leq \tau, \quad (2b)$$

$$\gamma_e = \arctan[(V \sin \gamma + W_h) / (V \cos \gamma + W_x)]. \quad (2c)$$

Here,  $t$  is the running time;  $\tau$  is the final time;  $\alpha$  is the angle of attack;  $\gamma_e$  is the absolute path inclination;  $\gamma_{e0}$  is the value at  $\gamma_e$  at  $t = 0$ ;  $\gamma$  is the relative path inclination;  $V$  is the relative velocity; and  $W_x$ ,  $W_h$  are the wind components [see Eqs. (1)].

This problem was studied under the assumption that maximum power setting is employed and that inequality constraints are imposed on the angle of attack and the angle of attack rate. Hence, the power setting  $\beta$  is such that

$$\beta = 1, \quad \dot{\beta} = 0, \quad (3a)$$

and the angle of attack  $\alpha$  is such that

$$\alpha \leq \alpha_*, \quad -\dot{\alpha}_* \leq \dot{\alpha} \leq \dot{\alpha}_*, \quad (3b)$$

where  $\alpha_*$  is the stick-shaker angle of attack and  $\dot{\alpha}_* = 3.0$  deg/sec is the limiting angle of attack rate.

With the above understanding, optimal trajectories were computed for three Boeing aircraft (B-727, B-737, and B-747) and several windshear intensities. From the extensive computations, certain general conclusions became apparent:

- (i) the optimal trajectories achieve minimum velocity at the end of the shear;
- (ii) the optimal trajectories require an initial decrease in the angle of attack, followed by a gradual increase; the maximum permissible angle of attack (stick-shaker angle of attack) is achieved near the end of the shear;
- (iii) for weak-to-moderate windshears, the optimal trajectories are characterized by a continuous climb; the average value of the path inclination decreases as the intensity of the shear increases;
- (iv) for relatively severe windshears, the optimal trajectories are characterized by an initial climb, followed by nearly-horizontal flight, followed by renewed climbing after the aircraft has passed through the shear region;
- (v) weak-to-moderate windshears and relatively severe windshears are survivable employing an optimized flight strategy; however, extremely severe windshears are not survivable, even employing an optimized flight strategy;

(vi) in relatively severe windshears, optimal trajectories have a better survival capability than maximum angle of attack trajectories and constant pitch trajectories.

For a particular case, the Boeing B-727 aircraft with a take-off weight  $W = 180000$  lb, a flap deflection  $\delta_F = 15$  deg, and an initial altitude  $h_0 = 50$  ft, optimal trajectories were computed for

$$\lambda = 0.8, 1.0, 1.1, \quad (4a)$$

corresponding to

$$\Delta W_x = 80, 100, 110 \text{ fps.} \quad (4b)$$

Figure 2 shows the resulting altitude profile  $h(t)$ , velocity profile  $V(t)$ , and angle of attack profile  $\alpha(t)$ . Clearly, as  $\Delta W_x$  increases, the altitude profile of the optimal trajectory changes: it is entirely ascending for  $\Delta W_x = 80$  fps; it includes a nearly-horizontal branch for  $\Delta W_x = 100$  fps; and it includes a descending branch for  $\Delta W_x = 110$  fps. Should the horizontal wind velocity difference be further increased to  $\Delta W_x = 120$  fps, the B-727 would crash, even flying an optimal take-off trajectory.

2.2. Guidance Trajectories. The computation of the optimal trajectories requires global information on the wind field; that is, it requires the knowledge of the wind components at every point of the region of space in which the aircraft is flying. In practice, global information is not available; even if it were available, there would not be enough computing

capability onboard and enough time to process it adequately. As a consequence, the optimal trajectories are merely benchmark trajectories that it is desirable to approach in actual flight.

Since global information is not available, what one can do is to employ local information on the wind field, in particular, local information on the wind acceleration and the downdraft. Therefore, the guidance problem must be addressed in these terms: Assuming that local information is available on the wind acceleration, the downdraft, as well as the state of the aircraft, we wish to guide an aircraft automatically or semiautomatically in such a way that the key properties of the optimal trajectories are preserved.

Based on the idea of preserving the properties of the optimal trajectories, three guidance schemes were developed at Rice University: (a) acceleration guidance, based on the relative acceleration; (b) absolute gamma guidance, based on the absolute path inclination; and (c) theta guidance, based on the pitch attitude angle. Among these, the acceleration guidance and the gamma guidance are of particular interest.

Key to all of the guidance schemes is the recognition of the fact that, in the shear region, the dynamical effects due to shear and downdraft can be combined into a single factor, called the shear/downdraft factor (Ref. 54),

$$F = \dot{W}_x/g - W_h/V. \quad (5)$$

The larger the value of  $F$ , the larger are the dynamical effects caused by the shear/downdraft combination.

In the acceleration guidance (AG), the guidance law has the form

$$(AG) \quad \dot{V}/g + C_1 F = 0; \quad (6)$$

therefore, it enforces the proportionality between the shear/downdraft factor and the instantaneous acceleration. In the gamma guidance (GG), the guidance law has the form

$$(GG) \quad \gamma_e - \gamma_{e0}(1 - C_2 F) = 0; \quad (7)$$

therefore, it enforces the achievement of decreasing values of the absolute path inclination with increasing values of the shear/downdraft factor. Note that (6) and (7) apply to the shear region.

In the aftershear region, guidance laws different from (6) and (7) are needed. Specifically, in the acceleration guidance (AG), partial velocity recovery is enforced,

$$(AG) \quad V - C_3 V_0 = 0. \quad (8)$$

In the gamma guidance (GG), partial path inclination recovery is enforced,

$$(GG) \quad \gamma_e - C_4 \gamma_{e0} = 0. \quad (9)$$

These guidance laws are then implemented via feedback control forms, such that the difference  $\alpha - \tilde{\alpha}$  is made proportional,

via suitable gain coefficients, to the violation of any of the guidance laws (6)-(9). Here,  $\alpha$  is the instantaneous angle of attack and  $\tilde{\alpha} = \tilde{\alpha}(V)$  is the nominal angle of attack.

Guidance trajectories were computed for the Boeing B-727 aircraft using the above guidance schemes. It was found that both the acceleration guidance (AG) and the gamma guidance (GG) produce trajectories which are close to the optimal trajectories (OT). In addition, the resulting near-optimal trajectories are superior to the trajectories arising from maximum angle of attack guidance (MAAG) and constant pitch guidance (CPG). See Fig. 3, which refers to the Boeing B-727 aircraft,  $\lambda = 1.0$ , and  $\Delta W_x = 100$  fps. While the MAAG trajectory crashes, the CPG trajectory scrapes the ground; on the other hand, the AG trajectory is close to the OT. An analogous remark holds for the GG trajectory, which is not shown, since it is nearly identical with the AG trajectory.

2.3. Simplified Guidance Trajectories. As stated above, the previous guidance schemes require local information on the wind acceleration, the downdraft, and the state of the aircraft. While this information will be available in future aircraft, it might not be available on current aircraft.

For current aircraft, one way to survive a windshear encounter is the quick horizontal flight transition technique, based on the properties of the optimal trajectories. The quick horizontal flight transition technique requires an initial decrease of the angle of attack, so as to decrease the path inclination to

nearly horizontal. Then, nearly-horizontal flight is maintained during the windshear encounter. Climbing flight is resumed after the shear is past.

For relatively severe windshears, the quick horizontal flight transition technique yields trajectories which are competitive with those of the guidance schemes discussed previously. In addition, for relatively severe windshears, the quick horizontal flight transition technique yields trajectories which have better survival capability than those resulting from maximum angle of attack guidance and constant pitch guidance.

2.4. Survival Capability. Perhaps, the best way of assessing the merit of a particular guidance scheme is the concept of survival capability. Consider the one parameter family of wind models (1). As the parameter  $\lambda$  increases, more intense windshear/downdraft combinations are generated until a critical value of  $\lambda$  is found (hence, a critical value of  $\Delta W_x$  is found), such that  $h_{\min} = 0$  for a given trajectory type. Thus, the survival capability is the critical wind velocity difference  $\Delta W_{xc}$  for which a crash first occurs.

The results are shown in Table 1, which supplies the survival capability  $\Delta W_{xc}$  for the optimal trajectory and various guidance trajectories. Table 1 also shows the windshear efficiency ratio  $\eta$ , defined to be

$$\eta = (\Delta W_{xc})_{PT} / (\Delta W_{xc})_{OT}. \quad (10)$$

Here, the subscript PT denotes a particular trajectory and the subscript OT denotes the optimal trajectory. Clearly, if the windshear efficiency of the OT is defined to be 100%, that of the AG trajectory is 95%, that of the GG trajectory is 96%, that of the CPG trajectory is 85%, and that of the MAAG trajectory is 48%.

### 3. Abort Landing Problem (Refs. 53, 57-59, 61-65)

3.1. Optimal Trajectories. Optimal abort landing trajectories were studied with the aid of the sequential gradient-restoration algorithm for optimal control problems. Several performance indexes were considered; the most reliable one was found to be the drop of altitude with respect to a reference value. Because the altitude drop has a maximum value along the flight path, attention was focused on minimizing the peak altitude drop. The resulting optimization problem is a minimax problem or Chebyshev problem of optimal control, in which the desired minimum performance index has the form

$$I_* = \min_{\alpha} I, \quad (11a)$$

$$I = \max_t |h_R - h|, \quad 0 \leq t \leq \tau. \quad (11b)$$

Here,  $t$  is the running time;  $\tau$  is the final time;  $\alpha$  is the angle of attack;  $h$  is the altitude above ground; and  $h_R$  is a reference value for the altitude, for instance  $h_R = h_* = 1000$  ft.

This problem was studied under the assumption that, at the windshear onset, the power setting  $\beta$  is increased from the initial value  $\beta = \beta_0$  to the maximum value  $\beta = 1$  at a constant time rate  $\dot{\beta} = \dot{\beta}_0$ ; afterward, the maximum value is kept. Inequality constraints are imposed on the angle of attack and the angle of attack rate. Hence,

$$\beta = \beta_0 + \dot{\beta}_0 t, \quad 0 \leq t \leq \sigma, \quad (12a)$$

$$\beta = 1, \quad \sigma \leq t \leq \tau, \quad (12b)$$

with  $\sigma = (1 - \beta_0)/\dot{\beta}_0$ , and

$$\alpha \leq \alpha_*, \quad -\dot{\alpha}_* \leq \dot{\alpha} \leq \dot{\alpha}_*, \quad (12c)$$

where  $\alpha_*$  is the stick-shaker angle of attack and  $\dot{\alpha}_* = 3.0$  deg/sec is the limiting angle of attack rate.

With the above understanding, optimal trajectories were computed for three Boeing aircraft (B-727, B-737, and B-747) and for several combinations of windshear intensity, initial altitude, and power setting rate. From the extensive computations, certain general conclusions became apparent with reference to strong-to-severe windshears:

- (i) the optimal trajectory includes three branches: a descending flight branch, followed by a nearly-horizontal flight branch, followed by an ascending flight branch after the aircraft has passed through the shear region;
- (ii) along an optimal trajectory, the point of minimum velocity is reached at the end of the shear;
- (iii) the peak altitude drop depends on the windshear intensity, the initial altitude, and the power setting rate; it increases as the windshear intensity increases and the initial altitude increases; and it decreases as the power setting rate increases;
- (iv) the peak altitude drop of the optimal trajectory is less than the peak altitude drop of the maximum

angle of attack trajectory and the constant pitch trajectory;

(v) the survival capability of the optimal trajectory is superior to that of the maximum angle of attack trajectory and the constant pitch trajectory.

For a particular case, the Boeing B-727 aircraft with a landing weight  $W = 150000$  lb, a flap deflection  $\delta_F = 30$  deg, and an initial altitude  $h_0 = 600$  ft, optimal trajectories were computed for

$$\lambda = 1.0, 1.2, 1.4, \quad (13a)$$

corresponding to

$$\Delta W_x = 100, 120, 140 \text{ fps.} \quad (13b)$$

Figure 4 shows the resulting altitude profile  $h(t)$ , velocity profile  $V(t)$ , and angle of attack profile  $\alpha(t)$ . Clearly, as  $\Delta W_x$  increases, the altitude profile of the optimal trajectory changes; in particular, as  $\Delta W_x$  increases, the minimum altitude of the optimal trajectory decreases, even though the aircraft still survives the windshear encounter. Should the horizontal wind velocity difference be further increased to  $\Delta W_x = 190$  fps, the B-727 would crash, even flying an optimal abort landing trajectory.

3.2. Guidance Trajectories. By necessity, guidance trajectories must rely on only local information on the wind acceleration, the downdraft, and the state of the aircraft. The intent is to guide an aircraft automatically or semi-automatically in such a way that the key properties of the

optimal trajectories are preserved.

Based on the idea of preserving the properties of the optimal trajectories, five guidance schemes were developed at Rice University: (a) target altitude guidance, based on the initial altitude and the total wind velocity difference; (b) safe target altitude guidance, based on only the initial altitude; (c) acceleration guidance, based on the relative acceleration; (d) gamma guidance, based on the absolute path inclination; and (e) theta guidance, based on two target pitch angles, a lower target pitch followed by a higher target pitch. Among these, the acceleration guidance and the gamma guidance are of particular interest.

Key to all of the guidance schemes is the recognition of the fact that, in the shear region, the dynamical effects due to shear and downdraft can be expressed via the shear/downdraft factor (Ref. 54)

$$F = \dot{W}_x/g - W_h/V. \quad (14)$$

The larger the value of  $F$ , the larger are the dynamical effects caused by the shear/downdraft combination.

In the acceleration guidance (AG), the guidance law has the form (6) for the shear region and the form (8) for the aftershear region. For the shear region, the constant  $C_1$  takes two values, one for the descending flight branch and one for the nearly-horizontal flight branch. Appropriate switch conditions regulate the transition from one branch to another of the AG trajectory.

In the gamma guidance (GG), the guidance law has the form (7) for the shear region and the form (9) for the aftershear region. For the shear region, the constant  $C_2$  takes two values, one for the descending flight branch and one for the nearly-horizontal flight branch. Appropriate switch conditions regulate the transition from one branch to another of the GG trajectory.

These guidance laws are then implemented via feedback control forms, such that the difference  $\alpha - \tilde{\alpha}$  is made proportional, via suitable gain coefficients, to the violation of any of the guidance laws (6)-(9). Here,  $\alpha$  is the instantaneous angle of attack and  $\tilde{\alpha} = \tilde{\alpha}(V)$  is the nominal angle of attack.

Guidance trajectories were computed for the Boeing B-727 aircraft using the above guidance schemes. It was found that both the acceleration guidance (AG) and the gamma guidance (GG) produce trajectories which are close to the optimal trajectories (OT). In addition, the resulting near-optimal trajectories are superior to the trajectories arising from maximum angle of attack guidance (MAAG) and constant pitch guidance (CPG). See Fig. 5, which refers to the Boeing B-727 aircraft,  $\lambda = 1.2$ , and  $\Delta W_x = 120$  fps. While the MAAG trajectory crashes, the CPG trajectory survives, albeit with a minimum altitude about half that of the OT. On the other hand, the AG trajectory is close to the OT. An analogous remark holds for the GG trajectory, which is not shown, since it is nearly identical with the AG trajectory.

3.3. Survival Capability. Perhaps, the best way of assessing the merit of a particular guidance scheme is the concept of survival capability. Consider the one-parameter family of wind models (1). As the parameter  $\lambda$  increases, more intense windshear/downdraft combinations are generated until a critical value of  $\lambda$  is found (hence, a critical value of  $\Delta W_x$  is found), such that  $h_{\min} = 0$  for a given trajectory type. Thus, the survival capability is the critical wind velocity difference  $\Delta W_{xc}$  for which a crash first occurs.

The results are shown in Table 2, which supplies the survival capability  $\Delta W_{xc}$  for the optimal trajectory and various guidance trajectories. Table 2 also shows the windshear efficiency ratio  $\eta$ , defined to be

$$\eta = (\Delta W_{xc})_{PT} / (\Delta W_{xc})_{OT} \quad (15)$$

Here, the subscript PT denotes a particular trajectory and the subscript OT denotes the optimal trajectory. Clearly, if the windshear efficiency of the OT is defined to be 100%, that of the AG trajectory is 96%, that of the GG trajectory is 98%, that of the CPG trajectory is 75%, and that of the MAAG trajectory is 44%.

#### 4. Penetration Landing Problem (Refs.55, 60, 62, 65)

4.1. Optimal Trajectories. Optimal penetration landing trajectories were studied with the aid of the sequential gradient-restoration algorithm for optimal control problems. The performance index being minimized is the least-square deviation of the flight trajectory from the nominal trajectory. The resulting optimization problem is a Bolza problem of optimal control, in which the desired minimum performance index has the form

$$I_* = \min_{\alpha, \beta} I, \quad (16a)$$

$$I = \int_0^{\tau} [h - \tilde{h}(x)]^2 dt. \quad (16b)$$

Here,  $t$  is the running time;  $\tau$  is the final time;  $\alpha$  is the angle of attack;  $\beta$  is the power setting;  $x$  is the horizontal distance;  $h$  is the altitude above ground; and  $\tilde{h}(x)$  is the nominal altitude. In turn, the function  $\tilde{h}(x)$  is computed by assuming that the nominal trajectory includes two parts: the approach part ( $h \geq 50$  ft), in which the slope  $\gamma_e$  is constant,  $\gamma_e = -3.0$  deg; and the flare part ( $h \leq 50$  ft), in which the slope  $\gamma_e$  is a linear function of the horizontal distance.

This problem was studied under the assumption that the absolute path inclination at touchdown is to be  $\gamma_e = -0.5$  deg; that the touchdown velocity is to be within  $\pm 30$  knots from the nominal value; and that the touchdown distance is to be within  $\pm 1000$  ft of the nominal value. Inequality constraints were imposed on the power setting, the power setting rate, the

angle of attack, and the angle of attack rate. Hence,

$$\beta_* \leq \beta \leq 1, \quad -\dot{\beta}_* \leq \dot{\beta} \leq \dot{\beta}_*, \quad (17a)$$

and

$$\alpha \leq \alpha_*, \quad -\dot{\alpha}_* \leq \dot{\alpha} \leq \dot{\alpha}_*. \quad (17b)$$

Here,  $\beta_*$  is the lower bound for the power setting;  $\dot{\beta}_*$  is the limiting power setting rate;  $\alpha_*$  is the stick-shaker angle of attack; and  $\dot{\alpha}_* = 3.0$  deg/sec is the limiting angle of attack rate.

With the above understanding, optimal trajectories were computed for the Boeing B-727 aircraft and for several combinations of windshear intensity, initial altitude, and power setting rate. From the extensive computations, certain general conclusions became apparent:

(i) the angle of attack has an initial decrease, which is followed by a gradual, sustained increase; the largest value of the angle of attack is attained near the end of the shear; in the aftershear region, the angle of attack decreases gradually;

(ii) initially, the power setting increases rapidly until maximum power setting is reached; then, maximum power setting is maintained in the shear region; in the aftershear region, the power setting decreases gradually;

(iii) the relative velocity decreases in the shear region and increases in the aftershear region; the point of minimum velocity occurs at the end of the shear;

(iv) depending on the windshear intensity and the initial altitude, the deviations of the flight trajectory from the nominal trajectory can be considerable in the shear region; however, these deviations become small in the aftershear region, and the optimal flight trajectory recovers the nominal trajectory;

(v) the optimal trajectory is better able to satisfy the touchdown requirements concerning the absolute path inclination, the velocity, and the distance than the fixed control trajectory (fixed angle of attack, coupled with fixed power setting) and the autoland trajectory (angle of attack controlled via path inclination signals, coupled with power setting controlled via velocity signals).

For a particular case, the Boeing B-727 aircraft with a landing weight  $W = 150000$  lb, a flap deflection  $\delta_F = 30$  deg, and an initial altitude  $h_0 = 600$  ft, optimal trajectories were computed for

$$\lambda = 1.0, 1.2, 1.4, \quad (18a)$$

corresponding to

$$\Delta W_x = 100, 120, 140 \text{ fps.} \quad (18b)$$

Figure 6 shows the resulting altitude profile  $h(x)$ , velocity profile  $V(x)$ , angle of attack profile  $\alpha(x)$ , and power setting profile  $\beta(x)$ .

4.2. Quasi-Optimal Trajectories. Quasi-optimal trajectories can be generated by minimizing the functional (16) under the

assumption that only one control is available, the angle of attack  $\alpha(t)$ , which is subject to Ineqs. (17b). The power setting  $\beta(t)$  is specified a priori, based on the results on the optimal trajectories.

For the shear portion of the trajectory, maximum power setting is maintained; that is, the function  $\beta(t)$  is given by

$$\beta = \beta_0 + \dot{\beta}_0 t, \quad 0 \leq t \leq \sigma, \quad (19a)$$

$$\beta = 1, \quad \sigma \leq t \leq \omega, \quad (19b)$$

with  $\sigma = (1 - \beta_0)/\dot{\beta}_0$ . Here,  $t = 0$  is the initial time,  $t = \sigma$  is the time at which maximum power setting is reached, and  $t = \omega$  is the time at which the shear terminates; also,  $\beta_0$  is the initial power setting and  $\dot{\beta}_0$  is the initial power setting rate.

For the aftershear portion of the trajectory, maximum power setting is maintained if  $V \leq V_\ell$  and reduced power setting is maintained if  $V > V_\ell$ , where  $V$  is the instantaneous relative velocity and  $V_\ell = V_0 - 30$  knots is the lower bound for the velocity. Hence,  $\beta(t)$  is supplied by the following relationship:

$$\beta - \beta_0 = (1 - \beta_0)(V_0 - V)/(V_0 - V_\ell), \quad (19c)$$

$$\beta_* \leq \beta \leq 1, \quad \omega \leq t \leq \tau. \quad (19d)$$

For a particular case, the Boeing B-727 aircraft with a landing weight  $W = 150000$  lb, a flap deflection  $\delta_F = 30$  deg, and an initial altitude  $h_0 = 600$  ft, quasi-optimal trajectories

were computed for the conditions (18). From the numerical results, upon comparing the optimal trajectory (OT), the quasi-optimal trajectory (QOT), and the nominal trajectory (NT), the following conclusions became apparent:

(i) the OT and the QOT are geometrically close to one another;

(ii) both the OT and the QOT are geometrically close to the NT, providing the windshear is not exceptionally severe,  $\Delta W_x \leq 120$  fps;

(iii) both the OT and the QOT satisfy the touchdown requirements concerning the absolute path inclination, the velocity, and the distance.

Results (i)-(iii) imply that, for the purposes of constructing a guidance scheme, the coupling relation between the angle of attack and the power setting can be ignored. This separation result simplifies to a considerable degree the design of guidance and control systems capable of approximating the behavior of the optimal penetration landing trajectory in the presence of windshear (Ref. 60).

4.3. Guidance Trajectories. A penetration landing guidance (PLG) scheme was constructed, based on the following ideas: to rely on only local information on the wind acceleration, the downdraft, and the state of the aircraft; to preserve the key properties of the optimal trajectories; to treat the power setting and the angle of attack as decoupled controls. Because of the separation result of the previous section, the power setting determination can be based on the velocity, while the angle

of attack determination can be based on the absolute path inclination and the glide slope.

For the power setting, the guidance law has the form

$$\beta - 1 = 0, \quad (20a)$$

in the shear portion of the trajectory. This means that the power setting must be increased as soon as possible to the maximum value.

Also for the power setting, the guidance law has the form

$$V - V_0 = 0, \quad (20b)$$

in the aftershear portion of the trajectory. This forces the achievement of velocities consistent with the velocity touchdown requirement.

The guidance laws (20) are then implemented via a single feedback control form, such that the difference  $\beta - \beta_0$  is a linear combination, via suitable gain coefficients, of two terms. The first term is proportional to the shear/downdraft factor  $F$  and takes care indirectly of (20a). The second term is proportional to the violation of the guidance law (20b); indeed, it is identical with the right-hand side of (19c).

For the angle of attack, the objective of the guidance law is to maintain the flight trajectory close to the nominal trajectory via two signals: the absolute path inclination  $\gamma_e$  and the glide slope  $\gamma_g$ .

For the approach part ( $h \geq 50\text{ft}$ ), the glide slope signals are predominant. Hence, the guidance law is dominated by

$$\gamma_g - \tilde{\gamma}_g(h,F) = 0. \quad (21a)$$

Here,  $\gamma_g$  is the instantaneous glide slope;  $\tilde{\gamma}_g$  is the nominal value of  $\gamma_g$ ;  $h$  is the instantaneous altitude; and  $F$  is the shear/downdraft factor. The function  $\tilde{\gamma}_g(h,F)$  is determined from the study of the optimal trajectories; for details, see Ref. 60. Enforcement of (21a) is essential to achieving the required touchdown distance.

For the flare part ( $h \leq 50$  ft), the absolute path inclination signals are predominant. Hence, the guidance law is dominated by

$$\gamma_e - \tilde{\gamma}_e(h,F) = 0. \quad (21b)$$

Here,  $\gamma_e$  is the instantaneous absolute path inclination;  $\tilde{\gamma}_e$  is the nominal value of  $\gamma_e$ ;  $h$  is the instantaneous altitude; and  $F$  is the shear/downdraft factor. The function  $\tilde{\gamma}_e(h,F)$  is determined from the study of the optimal trajectories; for details, see Ref. 60. Enforcement of (21b) is essential to achieving the required touchdown absolute path inclination.

The guidance laws (21) are then implemented via a feedback control form, such that the difference  $\alpha - \tilde{\alpha}$  is a linear combination, via suitable gain coefficients, of the violations of the guidance laws (21). Here,  $\alpha$  is the instantaneous angle of attack and  $\tilde{\alpha} = \tilde{\alpha}(V)$  is the nominal angle of attack.

Guidance trajectories were computed for the Boeing B-727 aircraft using the above guidance scheme. It was found that the penetration landing guidance (PLG) produces trajectories which are relatively close to the optimal trajectories (OT).

In addition, the resulting near-optimal trajectories are superior to the trajectories arising via fixed-control guidance (FCG) and autoland guidance (ALG) in terms of the ability to meet the touchdown requirements and in terms of survival capability in strong-to-severe windshears. See Fig. 7, which refers to the Boeing B-727 aircraft,  $\lambda = 1.2$ , and  $\Delta W_x = 120$  fps. Both the FCG trajectory and the ALG trajectory crash; however, the PLG trajectory survives the windshear encounter, just as the OT.

4.4. Simplified Guidance Trajectories. From a practical point of view, it must be emphasized that penetration landing makes sense only if the windshear encounter occurs at lower altitudes; if the windshear encounter occurs at higher altitudes, abort landing must be preferred. Therefore, low-altitude penetration landing deserves particular attention.

For this special situation,  $h_0 \leq 200$  ft, the guidance scheme of the previous section can be simplified by keeping the power setting at the maximum permissible value and by controlling the angle of attack via absolute path inclination signals. This is the same as stating that, among all the touchdown requirements, priority must be given to the touchdown path inclination requirement.

For the power setting, the guidance law has the form

$$\beta - 1 = 0, \tag{22}$$

which is now employed in both the shear portion and the aftershear portion of the trajectory. This means that the power setting must be increased as soon as possible to the maximum value and then kept at the maximum value until touchdown.

For the angle of attack, the objective of the guidance law is to maintain the flight trajectory close to the nominal trajectory via only path inclination signals. The guidance law has the form

$$\gamma_e - \tilde{\gamma}_e(h) = 0, \quad (23)$$

which differs from (21b) in that the nominal absolute path inclination does not involve the shear/downdraft factor. Therefore, the function  $\tilde{\gamma}_e(h)$  in (23) is the same as the function characterizing the nominal trajectory (NT); for details, see Ref. 60.

The guidance law (23) is then implemented via a feedback control form, such that the difference  $\alpha - \tilde{\alpha}$  is made proportional, via a suitable gain coefficient, to the violation of the guidance law (23). Here,  $\alpha$  is the instantaneous angle of attack and  $\tilde{\alpha} = \tilde{\alpha}(V)$  is the nominal angle of attack.

Simplified guidance trajectories were computed for the Boeing B-727 aircraft using the above guidance scheme. It was found that the simplified penetration landing guidance (SPLG) produces trajectories which are close to both the optimal trajectories (OT) and the nominal trajectories (NT). For detailed results, see Ref. 60..

##### 5. View Toward the Future

Over the past five years, considerable research has been performed at Rice University on two aspects of the windshear problem: determination of optimal trajectories and development of near-optimal guidance schemes. It now appears that, over the next 2-3 years, an advanced windshear control system can be developed, capable of functioning in different wind models and capable of covering the entire spectrum of flight conditions, including take-off, abort landing, and penetration landing.

The advanced windshear control system must combine an advanced windshear detection system and an advanced windshear recovery system. The advanced windshear detection system requires the use of real-time identification techniques and must be characterized by small computational time, coupled with limited memory requirements. The advanced windshear recovery system must incorporate four basic properties explained below: completeness, continuation, near-optimality, and simplicity.

Completeness means that the system should be able to function in take-off, abort landing, and penetration landing. Continuation means that the system should cover a variety of situations, ranging from zero windshear to moderate windshear to strong-to-severe windshear; the switch from no-windshear operation to windshear operation should be smooth. Near-optimality means that the system should be constructed so as to supply a good approximation to the properties of the optimal trajectories. Simplicity means that the system should be as simple as possible

and should emphasize the use of existing instrumentation, whenever possible.

With reference to the continuation property, it must be noted that any adverse wind gradient is both preceded and followed by a favorable wind gradient. The advanced windshear recovery system must not only react in a near-optimal way to adverse wind gradients, but must exploit to the best advantage of the aircraft favorable wind gradients. This means that, in an increasing headwind scenario, kinetic energy must be increased; conversely, in a decreasing tailwind scenario, potential energy must be increased. Clearly, this requires that not only the current windshear signals be measured, but that previous windshear signals be recorded and memorized, such that favorable wind gradients can be detected and utilized. Hence, some modification of the guidance schemes described in Sections 2-4 is in order.

To sum up, it is felt that an advanced windshear control system, endowed with the properties described above, should improve considerably the survival capability of the aircraft in a severe windshear.

## 6. Appendix A: Equations of Motion

In this report, we make use of the relative wind-axes system in connection with the following assumptions: (a) the aircraft is a particle of constant mass; (b) flight takes place in a vertical plane; (c) Newton's law is valid in an Earth-fixed system; and (d) the wind flow field is steady.

With the above premises, the equations of motion include the kinematical equations

$$\dot{x} = V \cos \gamma + W_x, \quad (24a)$$

$$\dot{h} = V \sin \gamma + W_h, \quad (24b)$$

and the dynamical equations

$$\begin{aligned} \dot{V} = & (T/m) \cos(\alpha + \delta) - D/m - g \sin \gamma \\ & - (\dot{W}_x \cos \gamma + \dot{W}_h \sin \gamma), \end{aligned} \quad (25a)$$

$$\begin{aligned} \dot{\gamma} = & (T/mV) \sin(\alpha + \delta) + L/mV - (g/V) \cos \gamma \\ & + (1/V) (\dot{W}_x \sin \gamma - \dot{W}_h \cos \gamma). \end{aligned} \quad (25b)$$

Because of assumption (d), the total derivatives of the wind velocity components and the corresponding partial derivatives satisfy the relations

$$\dot{W}_x = (\partial W_x / \partial x) (V \cos \gamma + W_x) + (\partial W_x / \partial h) (V \sin \gamma + W_h), \quad (26a)$$

$$\dot{W}_h = (\partial W_h / \partial x) (V \cos \gamma + W_x) + (\partial W_h / \partial h) (V \sin \gamma + W_h). \quad (26b)$$

These equations must be supplemented by the functional relations

$$T = T(h, V, \beta), \quad (27a)$$

$$D = D(h, V, \alpha), \quad L = L(h, V, \alpha), \quad (27b)$$

$$W_x = W_x(x, h), \quad W_h = W_h(x, h), \quad (27c)$$

and by the analytical relations

$$\theta = \alpha + \gamma, \quad (28a)$$

$$\gamma_e = \arctan[(V \sin \gamma + W_h) / (V \cos \gamma + W_x)]. \quad (28b)$$

The differential system (24)-(27) involves four state variables  $[x(t), h(t), V(t), \gamma(t)]$  and two control variables  $[\alpha(t), \beta(t)]$ . However, the number of control variables reduces to one (the angle of attack), if the power setting is specified in advance. The quantities (28) can be computed a posteriori, once the values of the state and the control are known.

7. Appendix B: Notations

Throughout the report, the following notations are employed:

D = drag force, lb;

F = shear/downdraft factor;

g = acceleration of gravity,  $\text{ft sec}^{-2}$ ;

h = altitude, ft;

L = lift force, lb;

m = mass,  $\text{lb ft}^{-1} \text{sec}^2$ ;

S = reference surface area,  $\text{ft}^2$ ;

t = running time, sec;

T = thrust force, lb;

V = relative velocity,  $\text{ft sec}^{-1}$ ;

W = mg = weight, lb;

$W_h$  = h-component of wind velocity,  $\text{ft sec}^{-1}$ ;

$W_x$  = x-component of wind velocity,  $\text{ft sec}^{-1}$ ;

x = horizontal distance, ft;

$\alpha$  = angle of attack (wing), rad;

$\beta$  = engine power setting;

$\gamma$  = relative path inclination, rad;

$\gamma_e$  = absolute path inclination, rad;

$\gamma_g$  = glide slope angle, rad;

$\delta$  = thrust inclination, rad;

$\delta_F$  = flap deflection, rad;

$\theta$  = pitch attitude angle (wing), rad;

$\lambda$  = wind intensity parameter;

$\tau$  = final time, sec.

References: Reports

1. MIELE, A., WANG, T., and MELVIN, W. W., Optimal Flight Trajectories in the Presence of Windshear, Part 1, Equations of Motion, Rice University, Aero-Astronautics Report No. 191, 1985.
2. MIELE, A., WANG, T., and MELVIN, W. W., Optimal Flight Trajectories in the Presence of Windshear, Part 2, Problem Formulation, Take-Off, Rice University, Aero-Astronautics Report No. 192, 1985.
3. MIELE, A., WANG, T., and MELVIN, W. W., Optimal Flight Trajectories in the Presence of Windshear, Part 3, Algorithms, Rice University, Aero-Astronautics Report No. 193, 1985.
4. MIELE, A., WANG, T., and MELVIN, W. W., Optimal Flight Trajectories in the Presence of Windshear, Part 4, Numerical Results, Take-Off, Rice University, Aero-Astronautics Report No. 194, 1985.
5. MIELE, A., Summary Report on NASA Grant No. NAG-1-516, Optimal Flight Trajectories in the Presence of Windshear, 1984-85, Rice University, Aero-Astronautics Report No. 195, 1985.
6. MIELE, A., WANG, T., and MELVIN, W. W., Guidance Strategies for Near-Optimum Performance in a Windshear, Part 1, Take-Off, Basic Strategies, Rice University, Aero-Astronautics Report No. 201, 1986.

7. MIELE, A., WANG, T., and MELVIN, W. W., Guidance Strategies for Near-Optimum Performance in a Windshear, Part 2, Take-Off, Comparison Strategies, Rice University, Aero-Astronautics Report No. 202, 1986.
8. MIELE, A., Summary Report on NASA Grant No. NAG-1-516, Optimal Flight Trajectories in the Presence of Windshear, 1984-86, Rice University, Aero-Astronautics Report No. 203, 1986.
9. MIELE, A., WANG, T., and MELVIN, W. W., Optimal Take-Off Trajectories in the Presence of Windshear, Rice University, Aero-Astronautics Report No. 206, 1986.
10. MIELE, A., WANG, T., and MELVIN, W. W., Guidance Strategies for Near-Optimum Take-Off Performance in a Windshear, Rice University, Aero-Astronautics Report No. 207, 1986.
11. MIELE, A., WANG, T., and MELVIN, W. W., Optimization and Acceleration Guidance of Flight Trajectories in a Windshear, Rice University, Aero-Astronautics Report No. 208, 1986.
12. MIELE, A., WANG, T., and MELVIN, W. W., Optimization and Gamma/Theta Guidance of Flight Trajectories in a Windshear, Rice University, Aero-Astronautics Report No. 209, 1986.
13. MIELE, A., WANG, T., and MELVIN, W. W., Quasi-Steady Flight to Quasi-Steady Flight Transition in a Wind-shear: Trajectory Optimization, Rice University, Aero-Astronautics Report No. 210, 1986.

14. MIELE, A., WANG, T., and MELVIN, W. W., Quasi-Steady Flight to Quasi-Steady Flight Transition in a Wind-shear: Trajectory Guidance, Rice University, Aero-Astronautics Report No. 211, 1986.
15. MIELE, A., WANG, T., and MELVIN, W. W., Gamma Guidance Schemes and Piloting Implications for Flight in a Windshear, Rice University, Aero-Astronautics Report No. 212, 1986.
16. MIELE, A., WANG, T., and MELVIN, W. W., Maximum Survival Capability of an Aircraft in a Severe Wind-shear, Rice University, Aero-Astronautics Report No. 213, 1986.
17. MIELE, A., WANG, T., TZENG, C. Y., and MELVIN, W. W., Optimal Abort Landing Trajectories in the Presence of Windshear, Rice University, Aero-Astronautics Report No. 215, 1987.
18. MIELE, A., WANG, T., WANG, H., and MELVIN, W. W., Optimal Penetration Landing Trajectories in the Presence of Windshear, Rice University, Aero-Astronautics Report No. 216, 1987.
19. MIELE, A., WANG, T., TZENG, C. Y., and MELVIN, W. W., Abort Landing Guidance Trajectories in the Presence of Windshear, Rice University, Aero-Astronautics Report No. 217, 1987.

20. MIELE, A., WANG, T., and MELVIN, W. W., Penetration Landing Guidance Trajectories in the Presence of Wind-shear, Rice University, Aero-Astronautics Report No. 218, 1987.
21. MIELE, A., WANG, T., and MELVIN, W. W., Quasi-Steady Flight to Quasi-Steady Flight Transition for Abort Landing in a Windshear: Trajectory Optimization and Guidance, Rice University, Aero-Astronautics Report No. 219, 1987.
22. MIELE, A., Research of the Aero-Astronautics Group of Rice University on the Windshear Problem, Rice University, Aero-Astronautics Report No. 221, 1987.
23. MIELE, A., WANG, T., and MELVIN, W. W., Gamma Guidance Schemes for Flight in a Windshear, Rice University, Aero-Astronautics Report No. 222, 1987.
24. MIELE, A., WANG, T., and MELVIN, W. W., Acceleration, Gamma, and Theta Guidance Schemes for Abort Landing Trajectories in the Presence of Windshear, Rice University, Aero-Astronautics Report No. 223, 1987.
25. MIELE, A., Summary Report on NASA Grant No. NAG-1-516, Optimization and Guidance of Flight Trajectories in the Presence of Windshear, 1984-87, Rice University, Aero-Astronautics Report No. 226, 1987.
26. MIELE, A., Perspectives on Windshear Research, Rice University, Aero-Astronautics Report No. 228, 1988.

27. MIELE, A., and WANG, H., Optimal Take-Off Trajectories of B-727, B-737, and B-747 Aircraft in the Presence of Windshear, Rice University, Aero-Astronautics Report No. 229, 1988.
28. MIELE, A., and WANG, H., Optimal Abort Landing Trajectories of B-727, B-737, and B-747 Aircraft in the Presence of Windshear, Rice University, Aero-Astronautics Report No. 230, 1988.
29. MIELE, A., WANG, H., TZENG, C. Y., and MELVIN, W. W., Optimal Recovery Techniques from High-Angle-of-Attack Windshear Encounters: Take-Off Problem, Rice University, Aero-Astronautics Report No. 236, 1989.
30. MIELE, A., WANG, H., TZENG, C. Y., and MELVIN, W. W., Optimal Recovery Techniques from High-Angle-of-Attack Windshear Encounters: Abort Landing Problem, Rice University, Aero-Astronautics Report No. 237, 1989.
31. MIELE, A., Final Report on NASA Grant No. NAG-1-516, Optimization and Guidance of Flight Trajectories in the Presence of Windshear, 1984-89, Rice University, Aero-Astronautics Report No. 244, 1989.

References: Scientific Meetings

32. MIELE, A., WANG, T., and MELVIN, W. W., Optimal Take-Off Trajectories in the Presence of Windshear, Paper No. AIAA-85-1843, AIAA Flight Mechanics Conference, Snowmass, Colorado, 1985.
33. MIELE, A., WANG, T., and MELVIN, W. W., Guidance Strategies for Near-Optimum Take-Off Performance in a Windshear, Paper No. AIAA-86-0181, AIAA 24th Aerospace Sciences Meeting, Reno, Nevada, 1986.
34. MIELE, A., WANG, T., and MELVIN, W. W., Optimization and Acceleration Guidance of Flight Trajectories in a Windshear, Paper No. AIAA-86-2036, AIAA Guidance, Navigation, and Control Conference, Williamsburg, Virginia, 1986.
35. MIELE, A., WANG, T., and MELVIN, W. W., Optimization and Gamma/Theta Guidance of Flight Trajectories in a Windshear, Paper No. ICAS-86-564, 15th Congress of the International Council of the Aeronautical Sciences, London, England, 1986.
36. MIELE, A., WANG, T., and MELVIN, W. W., Quasi-Steady Flight to Quasi-Steady Flight Transition in a Windshear: Trajectory Optimization, 6th IFAC Workshop on Control Applications of Nonlinear Programming and Optimization, London, England, 1986.

37. MIELE, A., WANG, T., and MELVIN, W. W., Quasi-Steady Flight to Quasi-Steady Flight Transition in a Windshear: Trajectory Guidance, Paper No. AIAA-87-0271, AIAA 25th Aerospace Sciences Meeting, Reno, Nevada, 1987.
38. MIELE, A., WANG, T., TZENG, C. Y., and MELVIN, W. W., Transformation Techniques for Minimax Optimal Control Problems and Their Application to Optimal Trajectories in a Windshear: Optimal Abort Landing Trajectories, Paper No. IFAC-87-9221, IFAC 10th World Congress, Munich, Germany, 1987.
39. MIELE, A., WANG, T., TZENG, C. Y., and MELVIN, W. W., Optimization and Guidance of Abort Landing Trajectories in a Windshear, Paper No. AIAA-87-2341, AIAA Guidance, Navigation, and Control Conference, Monterey, California, 1987.
40. MIELE, A., Primal-Dual Sequential Gradient Restoration Algorithms for Optimal Control Problems and Their Application to Flight in a Windshear, Proceedings of the International Conference on Optimization Techniques and Applications, Edited by K. L. Teo et al, Kent Ridge, Singapore, pp. 53-94, 1987.
41. MIELE, A., WANG, T., WANG, H., and MELVIN, W. W., Optimal Penetration Landing Trajectories in the Presence of Windshear, Paper No. AIAA-88-0580, AIAA 26th Aerospace Sciences Meeting, Reno, Nevada, 1988.

42. MIELE, A., WANG, T., and MELVIN, W. W., Optimization and Guidance of Landing Trajectories in a Windshear, Paper No. ICAS-88-332, 16th Congress of the International Council of the Aeronautical Sciences, Jerusalem, Israel, 1988.
43. MIELE, A., WANG, T., and MELVIN, W. W., Optimization and Guidance of Penetration Landing Trajectories in a Windshear, Paper Presented at the American Control Conference, Atlanta, Georgia, 1988.
44. MIELE, A., and WANG, T., Optimal Trajectories for Flight in a Windshear: Take-Off, Abort Landing, and Penetration Landing, Paper No. IMACS-88-352, 12th IMACS World Congress on Scientific Computation, Paris, France, 1988.
45. MIELE, A., WANG, T., and MELVIN, W. W., Penetration Landing Guidance Trajectories in the Presence of Windshear, Paper No. AIAA-88-4069, AIAA Guidance, Navigation, and Control Conference, Minneapolis, Minnesota, 1988.
46. MIELE, A., and WANG, T., Optimization Problems for Aircraft Flight in a Windshear, International School of Mathematics G. Stampacchia, Course on Nonsmooth Optimization and Related Topics, Erice, Italy, 1988.
47. MIELE, A., WANG, T., WANG, H., and MELVIN, W. W., Overview of Optimal Trajectories for Flight in a Windshear, Paper No. AIAA-89-0812, AIAA 27th Aerospace Sciences Meeting, Reno, Nevada, 1989.
48. MIELE, A., Advances in Windshear Recovery Research, 8th IFAC Workshop on Control Applications of Nonlinear Programming and Optimization, Paris, France, 1989.

References: Articles

49. MIELE, A., WANG, T., and MELVIN, W. W., Optimal Take-Off Trajectories in the Presence of Windshear, Journal of Optimization Theory and Applications, Vol. 49, No. 1, pp. 1-45, 1986.
50. MIELE, A., WANG, T., and MELVIN, W. W., Guidance Strategies for Near-Optimum Take-Off Performance in a Windshear, Journal of Optimization Theory and Applications, Vol. 50, No. 1, pp. 1-47, 1986.
51. MIELE, A., WANG, T., MELVIN, W.W., and BOWLES, R. L., Maximum Survival Capability of an Aircraft in a Severe Windshear, Journal of Optimization Theory and Applications, Vol. 53, No. 2, pp. 181-217, 1987.
52. MIELE, A., WANG, T., and MELVIN, W. W., Quasi-Steady Flight to Quasi-Steady Flight Transition in a Windshear: Trajectory Optimization and Guidance, Journal of Optimization Theory and Applications, Vol. 54, No. 2, pp. 203-240, 1987.
53. MIELE, A., WANG, T., and MELVIN, W. W., Optimal Abort Landing Trajectories in the Presence of Windshear, Journal of Optimization Theory and Applications, Vol. 55, No. 2, pp. 165-202, 1987.
54. MIELE, A., WANG, T., and MELVIN, W. W., Optimization and Acceleration Guidance of Flight Trajectories in a Windshear, Journal of Guidance, Control, and Dynamics, Vol. 10, No. 4, pp. 368-377, 1987.

55. MIELE, A., WANG, T., WANG, H., and MELVIN, W. W., Optimal Penetration Landing Trajectories in the Presence of Windshear, Journal of Optimization Theory and Applications, Vol. 57, No. 1, pp. 1-40, 1988.
56. MIELE, A., WANG, T., MELVIN, W. W., and BOWLES, R.L., Gamma Guidance Schemes for Flight in a Windshear, Journal of Guidance, Control, and Dynamics, Vol. 11, No. 4, pp. 320-327, 1988.
57. MIELE, A., WANG, T., and MELVIN, W. W., Quasi-Steady Flight to Quasi-Steady Flight Transition for Abort Landing in a Windshear: Trajectory Optimization and Guidance, Journal of Optimization Theory and Applications, Vol. 58, No. 2, pp. 165-207, 1988.
58. MIELE, A., WANG, T., TZENG, C. Y., and MELVIN, W. W., Abort Landing Guidance Trajectories in the Presence of Windshear, Journal of the Franklin Institute, Vol. 326, No. 2, pp. 185-220, 1989.
59. MIELE, A., WANG, T., MELVIN, W. W., and BOWLES, R. L., Acceleration, Gamma, and Theta Guidance for Abort Landing in a Windshear, Journal of Guidance, Control, and Dynamics, Vol. 12, No. 6, pp. 815-821, 1989.
60. MIELE, A., WANG, T., and MELVIN, W. W., Penetration Landing Guidance Trajectories in the Presence of Windshear, Journal of Guidance, Control, and Dynamics, Vol. 12, No. 6, pp. 806-814, 1989.

61. MIELE, A., Optimal Trajectories of Aircraft and Spacecraft, Aircraft Trajectories: Computation, Prediction, and Control, Edited by A. Benoit, AGARDograph No. AG-301, AGARD/NATO, Paris, France, Vol. 1, pp. xxx-xxx, 1989.
62. MIELE, A., and WANG, T., Optimization Problems for Aircraft Flight in a Windshear, Nonsmooth Optimization and Related Topics, Edited by F. H. Clarke, V.F. Demyanov, and F. Giannessi, Plenum Publishing Corporation, New York, New York, pp. 277-305, 1989.
63. MIELE, A., WANG, T., WANG, H., and MELVIN, W.W., Overview of Optimal Trajectories for Flight in a Windshear, Control and Dynamic Systems, Advances in Theory and Application, Edited by C. T. Leondes, Vol. 34, pp. xxx-xxx, 1989.
64. MIELE, A., WANG, T., and WU, G. D., Perspectives on Windshear Flight, Recent Advances in Aerospace Propulsion, Edited by G. Angelino, L. De Luca, and W. A. Sirignano, Springer-Verlag, Berlin, Germany, pp. xxx-xxx, 1989.
65. MIELE, A., Advances in Windshear Recovery Research, Proceedings of the 8th IFAC Workshop on Control Applications of Nonlinear Programming and Optimization, Edited by H. B. Siguerdidjane et al, IFAC Publications, Oxford, England, pp. xxx-xxx, 1989.

Supplementary Bibliography

66. MIELE, A., Flight Mechanics, Vol. 1, Theory of Flight Paths, Addison-Wesley Publishing Company, Reading, Massachusetts, 1962.
67. GERA, J., The Influence of Vertical Wind Gradients on the Longitudinal Motion of Airplanes, NASA, Technical Note No. D-6430, 1971.
68. HOUBOLT, J., Survey on Effect of Surface Winds on Aircraft Design and Operations and Recommendations for Needed Wind Research, NASA, Contractor Report No. 2360, 1973.
69. REEVES, P. M., et al, Development and Applications of a Nongaussian Atmospheric Turbulence Model for Use in Flight Simulators, NASA, Contractor Report No. 2451, 1974.
70. GOFF, R. C., Vertical Structure of Thunderstorm Outflows, Monthly Weather Review, Vol. 104, No. xx, pp. xxx-xxx, 1976.
71. ABZUG, M. J., Airspeed Stability under Windshear Conditions, Journal of Aircraft, Vol. 14, No. xx, pp. xxx-xxx, 1977.
72. FUJITA, T. T., and CARACENA, F., An Analysis of Three Weather-Related Aircraft Accidents, Bulletin of the American Meteorological Society, Vol. 58, No. xx, pp. xxx-xxx, 1977.
73. GOFF, R. C., Some Observations of Thunderstorm-Induced Low-Level Wind Variations, Journal of Aircraft, Vol. 14, No. xx, pp. xxx-xxx, 1977.
74. LEHMAN, J. M., HEFFLEY, R. K., and CLEMENT, W. F., Simulation and Analysis of Windshear Hazard, Federal Aviation Administration, Report No. FAA-RD-78-7, 1977.

75. SOWA, D. F., The Effect of Terrain near Airports on Significant Low-Level Windshear, Paper Presented at the AIAA Aircraft Systems and Technology Conference, Seattle, Washington, 1977.
76. FROST, W., and RAVIKUMAR, R., Investigation of Aircraft Landing in Variable Wind Fields, NASA, Contractor Report No. 3073, 1978.
77. FROST, W., and CROSBY, B., Investigations of Simulated Aircraft Flight through Thunderstorm Outflows, NASA, Contractor Report No. 3052, 1978.
78. MCCARTHY, J., BLICK, E. F., and BENSCH, R. R., Jet Transport Performance in Thunderstorm Windshear Conditions, NASA, Contractor Report No. 3207, 1979.
79. FUJITA, T. T., Downbursts and Microbursts: An Aviation Hazard, Paper Presented at the 9th AMS Conference on Radar Meteorology, Miami, Florida, 1980.
80. GERA, J., Longitudinal Stability and Control in Windshear with Energy Height Rate Feedback, NASA, Technical Memorandum No. 81828, 1980.
81. TURKEL, B. S., and FROST, W., Pilot-Aircraft System Response to Windshear, NASA, Contractor Report No. 3342, 1980.
82. WANG, S. T., and FROST, W., Atmospheric Turbulence Simulation Techniques with Application to Flight Analysis, NASA, Contractor Report No. 3309, 1980.
83. DANIEL, J., and FROST, W., 1981 Current Research on Aviation Weather (Bibliography), NASA, Contractor Report No. 3527, 1982.

84. HAINES, P. A., and LUERS, J. K., Aerodynamic Penalties of Heavy Rain on a Landing Aircraft, NASA, Contractor Report No. 156885, 1982.
85. MCCARTHY, J., and NORVIEL, V., Numerical and Flight Simulator Test of the Flight Deterioration Concept, NASA, Contractor Report No. 3500, 1982.
86. ANONYMOUS, N. N., Low Altitude Windshear and Its Hazard to Aviation, National Academy Press, Washington, DC, 1983.
87. ANONYMOUS, N. N., Aircraft Accident Report: Pan American World Airways, Clipper 759, Boeing 727-235, N4737, New Orleans International Airport, Kenner, Louisiana, July 9, 1982, Report No. NTSB-AAR-8302, National Transportation Safety Board, Washington, DC, 1983.
88. CARACENA, F., FLUECK, J. A., and MCCARTHY, J., Forecasting the Likelihood of Microbursts along the Front Range of Colorado, Paper Presented at the 13th AMS Conference on Severe Local Storms, Tulsa, Oklahoma, 1983.
89. FROST, W., Flight in Low-Level Windshear, NASA, Contractor Report No. 3678, 1983.
90. ZHU, S. X., and ETKIN, B., Fluid-Dynamic Model of a Downburst, University of Toronto, Institute for Aerospace Studies, Report No. UTIAS-271, 1983.
91. ALEXANDER, M. B., and CAMP, D. W., Wind Speed and Direction Shears with Associated Vertical Motion during Strong Surface Winds, NASA, Technical Memorandum No. 82566, 1984.

92. CAMPBELL, C. W., A Spatial Model of Windshear and Turbulence for Flight Simulation, NASA, Technical Paper No. 2313, 1984.
93. FROST, W., and BOWLES, R. L., Windshear Terms in the Equations of Aircraft Motion, Journal of Aircraft, Vol. 21, No. 11, pp. 866-872, 1984.
94. FROST, W., CHANG, H. P., ELMORE, K. L., and MCCARTHY, J., Simulated Flight through JAWS Windshear: In-Depth Analysis Results, Paper No. AIAA-84-0276, AIAA 22nd Aerospace Sciences Meeting, Reno, Nevada, 1984.
95. PSIAKI, M. L., and STENGEL, R. F., Analysis of Aircraft Control Strategies for Microburst Encounter, Paper No. AIAA-84-0238, AIAA 22nd Aerospace Sciences Meeting, Reno, Nevada, 1984.
96. ANONYMOUS, N. N., Flight Path Control in Windshear, Boeing Airliner, pp. 1-12, January-March, 1985.
97. FUJITA, T. T., The Downburst, Department of Geophysical Sciences, University of Chicago, Chicago, Illinois, 1985.
98. ZHU, S., and ETKIN, B., Model of the Wind Field in a Downburst, Journal of Aircraft, Vol. 22, No. 7, pp. 595-601, 1985.
99. ANONYMOUS, N. N., Aircraft Accident Report: Delta Air Lines, Lockheed L-1011-3851, N726DA, Dallas-Fort Worth International Airport, Texas, August 2, 1985, Report No. NTSB-AAR-8605, National Transportation Safety Board, Washington, DC, 1986.

100. BACH, R. E., and WINGROVE, R. C., The Analysis of Airline Flight Records for Winds and Performance with Application to the Delta 191 Accident, Paper No. AIAA-86-2227, AIAA Atmospheric Flight Mechanics Conference, Williamsburg, Virginia, 1986.
101. BRAY, R. S., Aircraft Performance and Control in Downburst Windshear, Paper No. SAE-86-1698, SAE Aerospace Technology Conference and Exposition, Long Beach, California, 1986.
102. FUJITA, T. T., DFW Microburst, Department of Geophysical Sciences, University of Chicago, Chicago, Illinois, 1986.
103. HAHN, K. U., Take-Off and Landing in a Downburst, Paper No. ICAS-86-562, 15th Congress of the International Council of the Aeronautical Sciences, London, England, 1986.
104. IVAN, M., A Ring-Vortex Downburst Model for Flight Simulation, Journal of Aircraft, Vol. 23, No. 3, pp. 232-236, 1986.
105. MELVIN, W. W., A New Look at Piloting Procedures in Microbursts, Paper No. SAE-86-1701, SAE Aerospace Technology Conference and Exposition, Long Beach, California, 1986.
106. MULALLY, A. R., and HIGGINS, C. R., Atmospheric Disturbances Affecting Safety of Flight, General Lecture, 15th Congress of the International Council of the Aeronautical Sciences, London, England, 1986.
107. PSIAKI, M. L., and STENGEL, R. F., Optimal Flight Paths through Microburst Wind Profiles, Journal of Aircraft, Vol. 23, No. 8, pp. 629-635, 1986.

108. ANONYMOUS, N. N., Windshear Training Aid, Vols. 1 and 2, Federal Aviation Administration, Washington, DC, 1987.
109. CHU, P. Y., and BRYSON, A. E., Jr., Control of Aircraft Landing Approach in Windshear, Paper No. AIAA-87-0632, AIAA 25th Aerospace Sciences Meeting, Reno, Nevada, 1987.
110. GORNEY, J. L., An Analysis of the Delta 191 Windshear Accident, Paper No. AIAA-87-0626, AIAA 25th Aerospace Sciences Meeting, Reno, Nevada, 1987.
111. WINGROVE, R. C., and BACH, R. E., Jr., Severe Winds in the DFW Microburst Measured from Two Aircraft, Paper No. AIAA-87-2340, AIAA Guidance, Navigation, and Control Conference, Monterey, California, 1987.
112. OSEGUERA, R. M., and BOWLES, R. L., A Simple, Analytic 3-Dimensional Downburst Model Based on Boundary-Layer Stagnation Flow, NASA, Technical Memorandum No. 100632, 1988.
113. HINTON, D. A., Piloted-Simulation Evaluation of Recovery Guidance for Microburst Windshear Encounters, NASA, Technical Paper No. 2886, 1989.
114. WINGROVE, R. C., and BACH, R. E., Jr., Severe Winds in the Dallas-Fort Worth Microburst Measured from Two Aircraft, Journal of Aircraft, Vol. 26, No. 3, pp. 221-224, 1989.
115. DOVIAK, R. J., and CHRISTIE, D. R., Thunderstorm Generated Solitary Waves: A Windshear Hazard, Journal of Aircraft, Vol. 26, No. 5, pp. 423-431, 1989.

116. VICROY, D. D., and BOWLES, R. L., Effect of Spatial Wind Gradients on Airplane Aerodynamics, Journal of Aircraft, Vol. 26, No. 6, pp. 523-530, 1989.
117. CHEN, Y. H., and PANDEY, S., Robust Control Strategy for Take-Off Performance in a Windshear, Optimal Control Applications and Methods, Vol. 10, No. 1, pp. 65-80, 1989.

List of Tables

Table 1. Take-off survival capability for the B-727 aircraft,

$W = 180000 \text{ lb}$ ,  $\delta_F = 15 \text{ deg}$ ,  $h_0 = 50 \text{ ft}$ .

Table 2. Abort landing survival capability for the B-727 aircraft,

$W = 150000 \text{ lb}$ ,  $\delta_F = 30 \text{ deg}$ ,  $h_0 = 600 \text{ ft}$ .

List of Captions

- Fig. 1A. Horizontal wind  $W_x$ .
- Fig. 1B. Vertical wind  $W_h$ .
- Fig. 2A. Take-off, optimal trajectories,  
altitude  $h$  versus time  $t$ .
- Fig. 2B. Take-off, optimal trajectories,  
velocity  $V$  versus time  $t$ .
- Fig. 2C. Take-off, optimal trajectories,  
angle of attack  $\alpha$  versus time  $t$ .
- Fig. 3. Take-off, guidance trajectories,  
altitude  $h$  versus time  $t$ .
- Fig. 4A. Abort landing, optimal trajectories,  
altitude  $h$  versus time  $t$ .
- Fig. 4B. Abort landing, optimal trajectories,  
velocity  $V$  versus time  $t$ .
- Fig. 4C. Abort landing, optimal trajectories,  
angle of attack  $\alpha$  versus time  $t$ .
- Fig. 5. Abort landing, guidance trajectories,  
altitude  $h$  versus time  $t$ .
- Fig. 6A. Penetration landing, optimal trajectories,  
altitude  $h$  versus time  $t$ .
- Fig. 6B. Penetration landing, optimal trajectories,  
velocity  $V$  versus time  $t$ .
- Fig. 6C. Penetration landing, optimal trajectories,  
angle of attack  $\alpha$  versus time  $t$ .

Fig. 6D. Penetration landing, optimal trajectories,  
power setting  $\beta$  versus time  $t$ .

Fig. 7. Penetration landing, guidance trajectories,  
altitude  $h$  versus time  $t$ .

Table 1. Take-off survival capability for the B-727 aircraft,  
 $W = 180000$  lb,  $\delta_F = 15$  deg,  $h_0 = 50$  ft.

Trajectory	$\lambda_c$	$\Delta W_{xc}$ (fps)	$\eta$
OT	1.195	119.5	1.000
AG	1.130	113.0	0.946
GG	1.153	115.3	0.965
CPG	1.018	101.8	0.852
MAAG	0.577	57.7	0.483

Table 2. Abort landing survival capability for the B-727 aircraft,  
 $W = 150000$  lb,  $\delta_F = 30$  deg,  $h_0 = 600$  ft.

Trajectory	$\lambda_c$	$\Delta W_{xc}$ (fps)	$\eta$
OT	1.871	187.1	1.000
AG	1.791	179.1	0.957
GG	1.842	184.2	0.985
CPG	1.394	139.4	0.745
MAAG	0.817	81.7	0.437

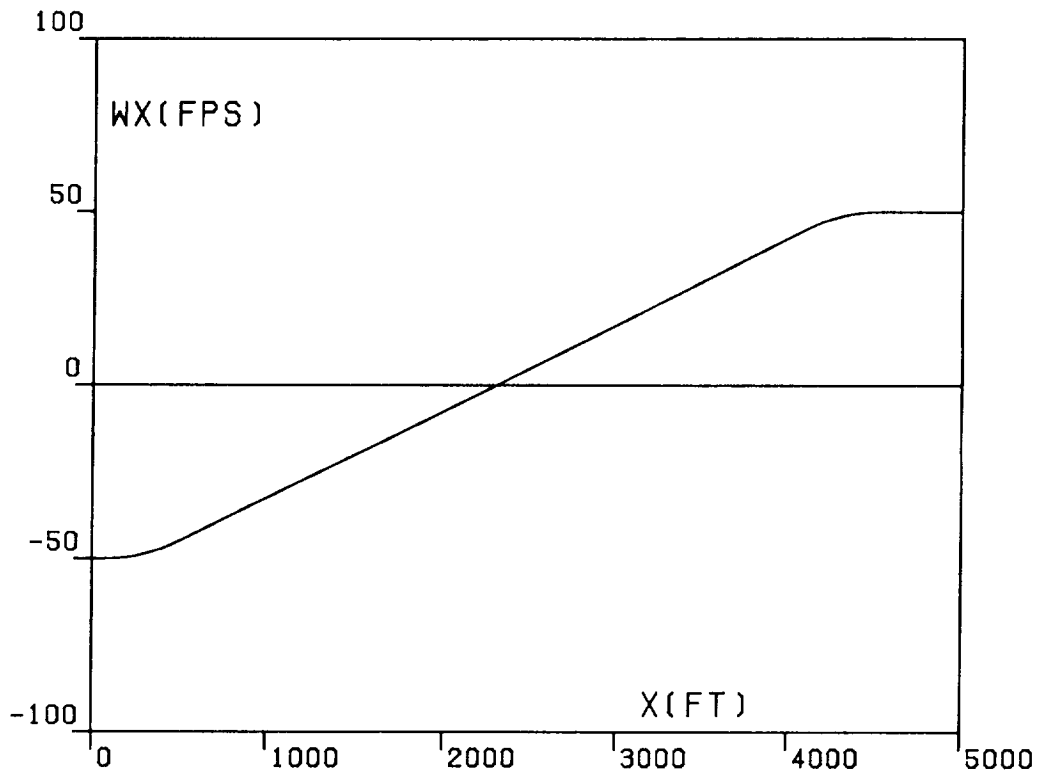


FIG.1A. HORIZONTAL WIND.

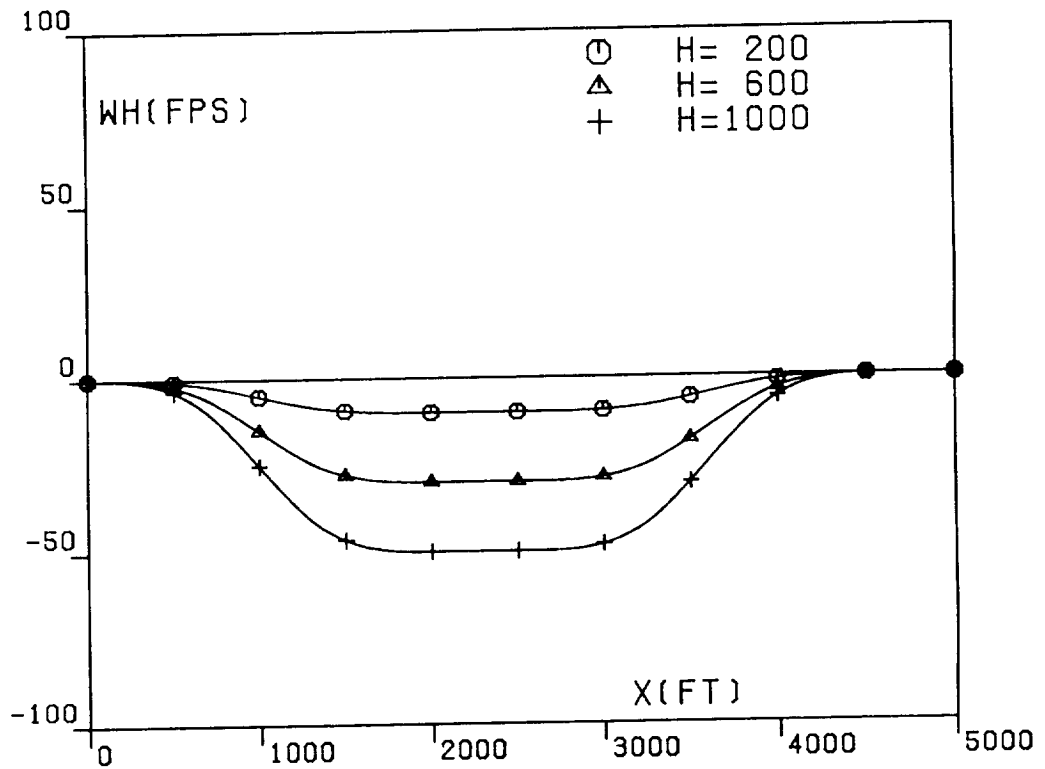


FIG.1B. VERTICAL WIND.

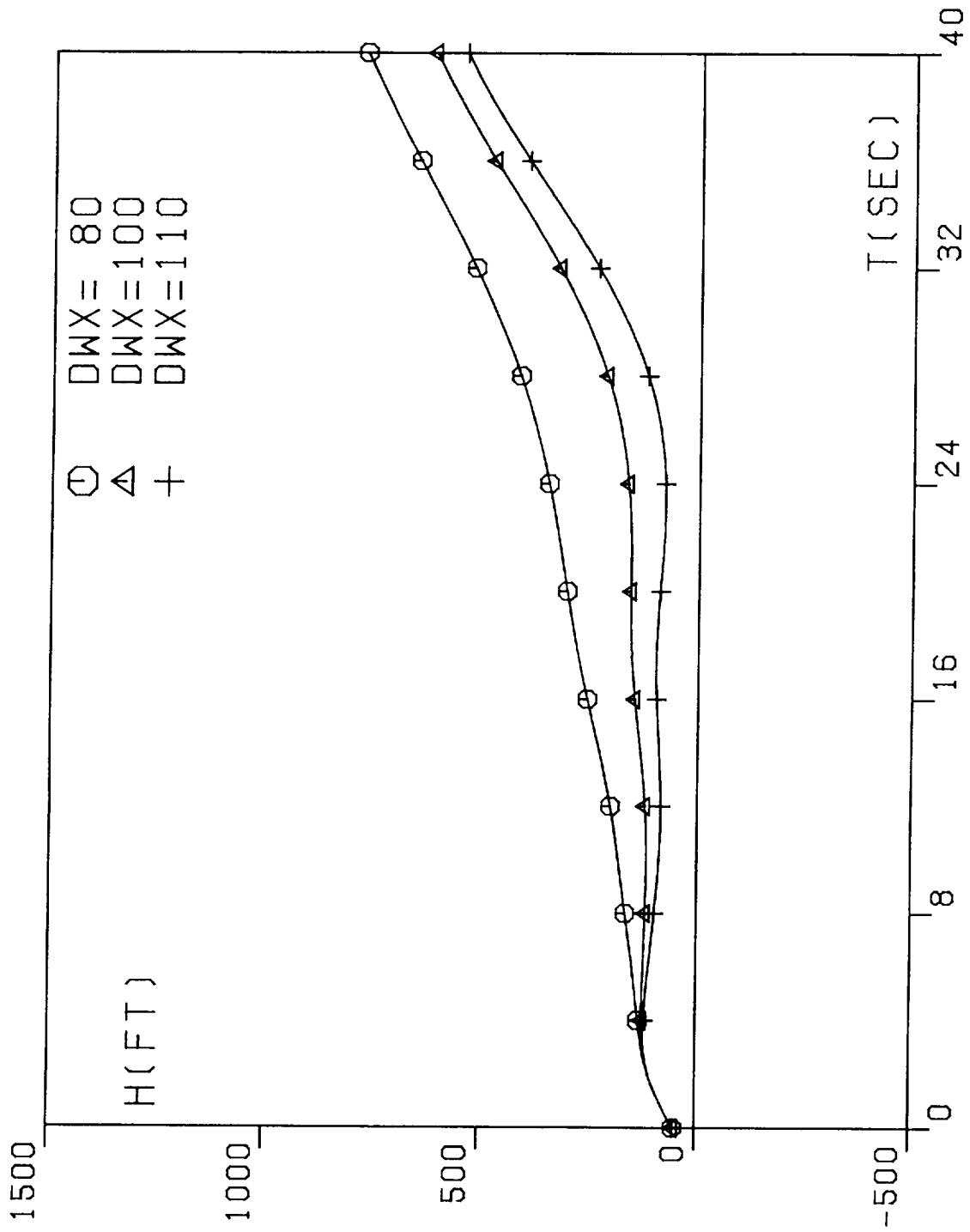


FIG. 2A. OPTIMAL TRAJECTORIES, TAKE-OFF.

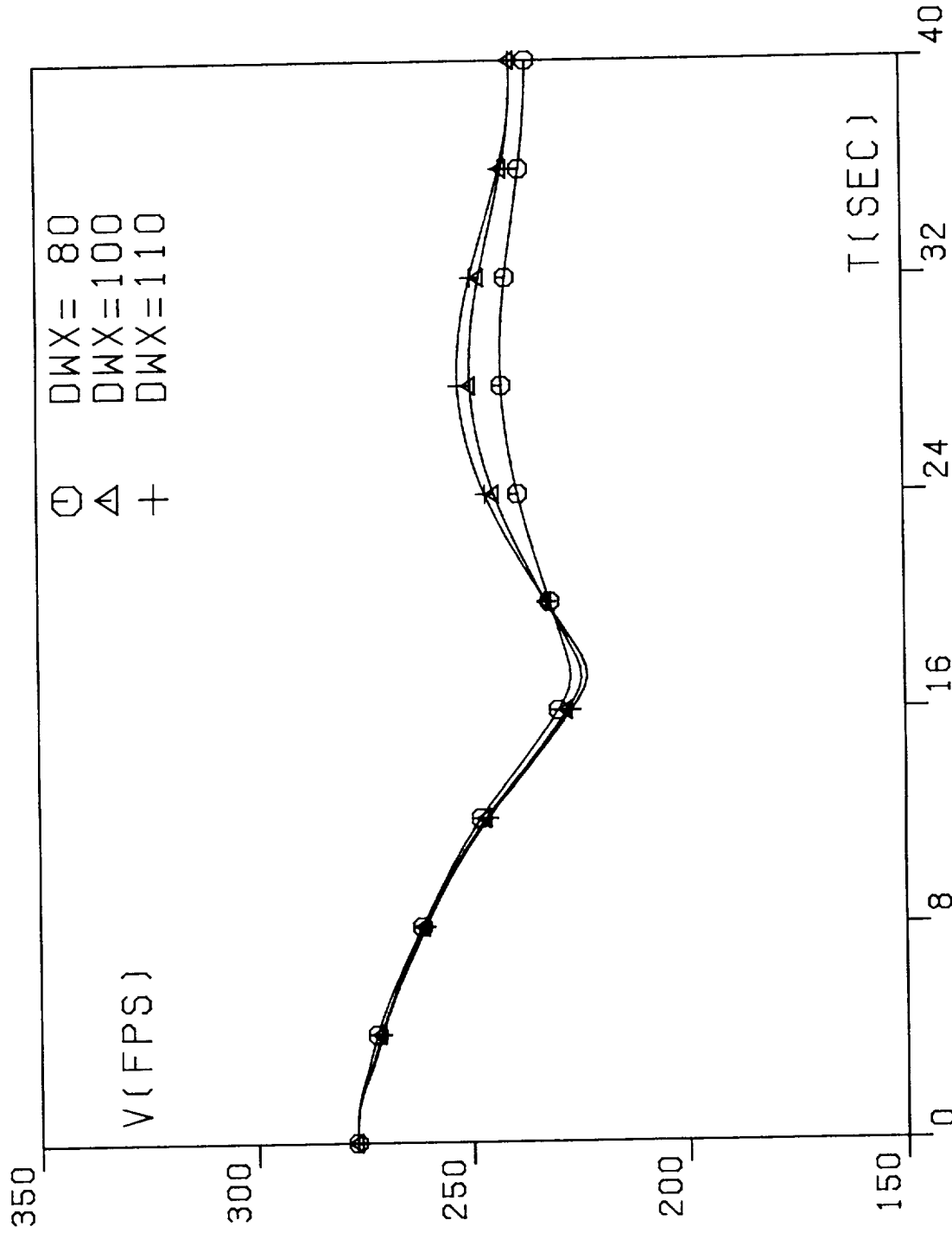


FIG. 2B. OPTIMAL TRAJECTORIES, TAKE-OFF.

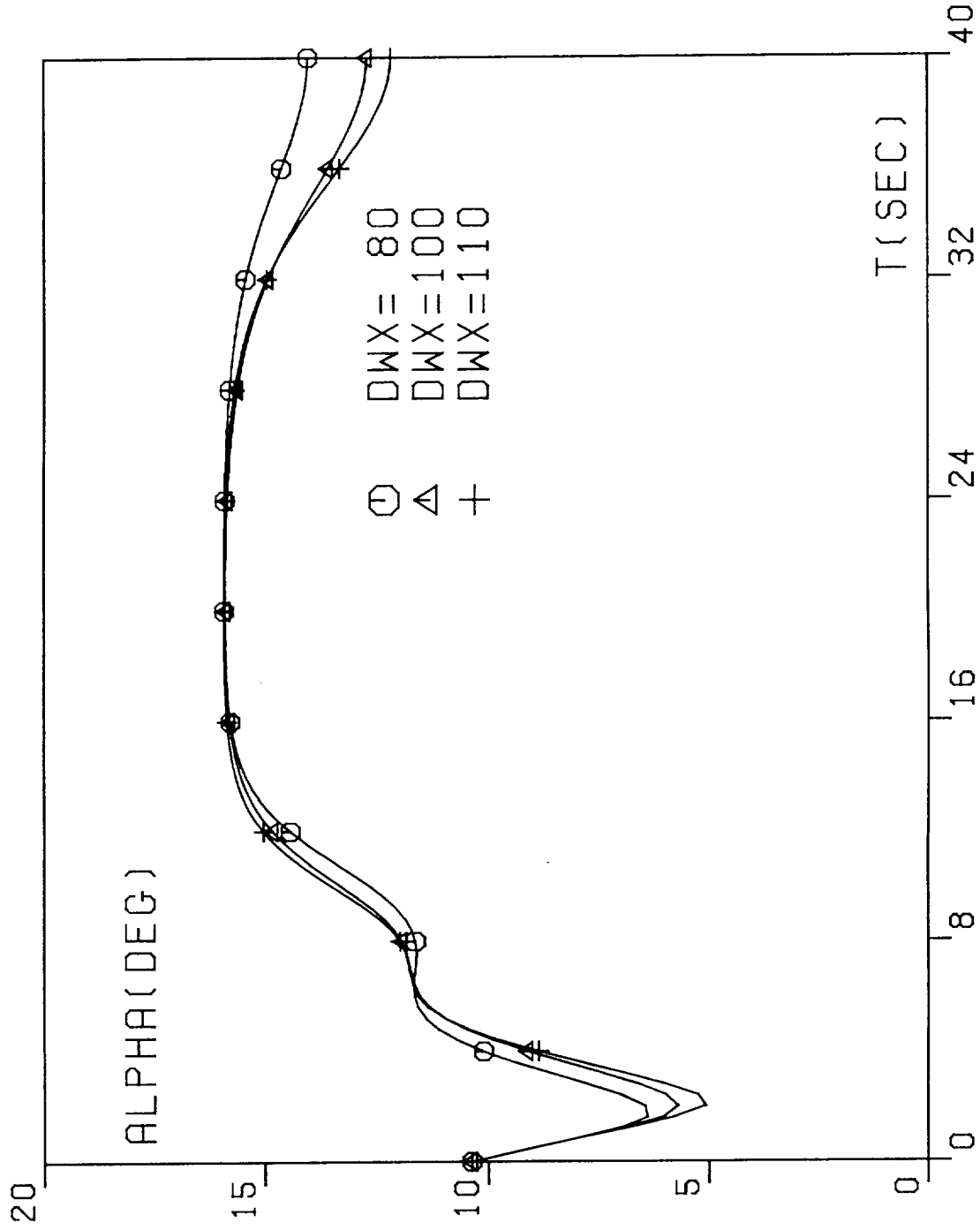


FIG. 2C. OPTIMAL TRAJECTORIES, TAKE-OFF.

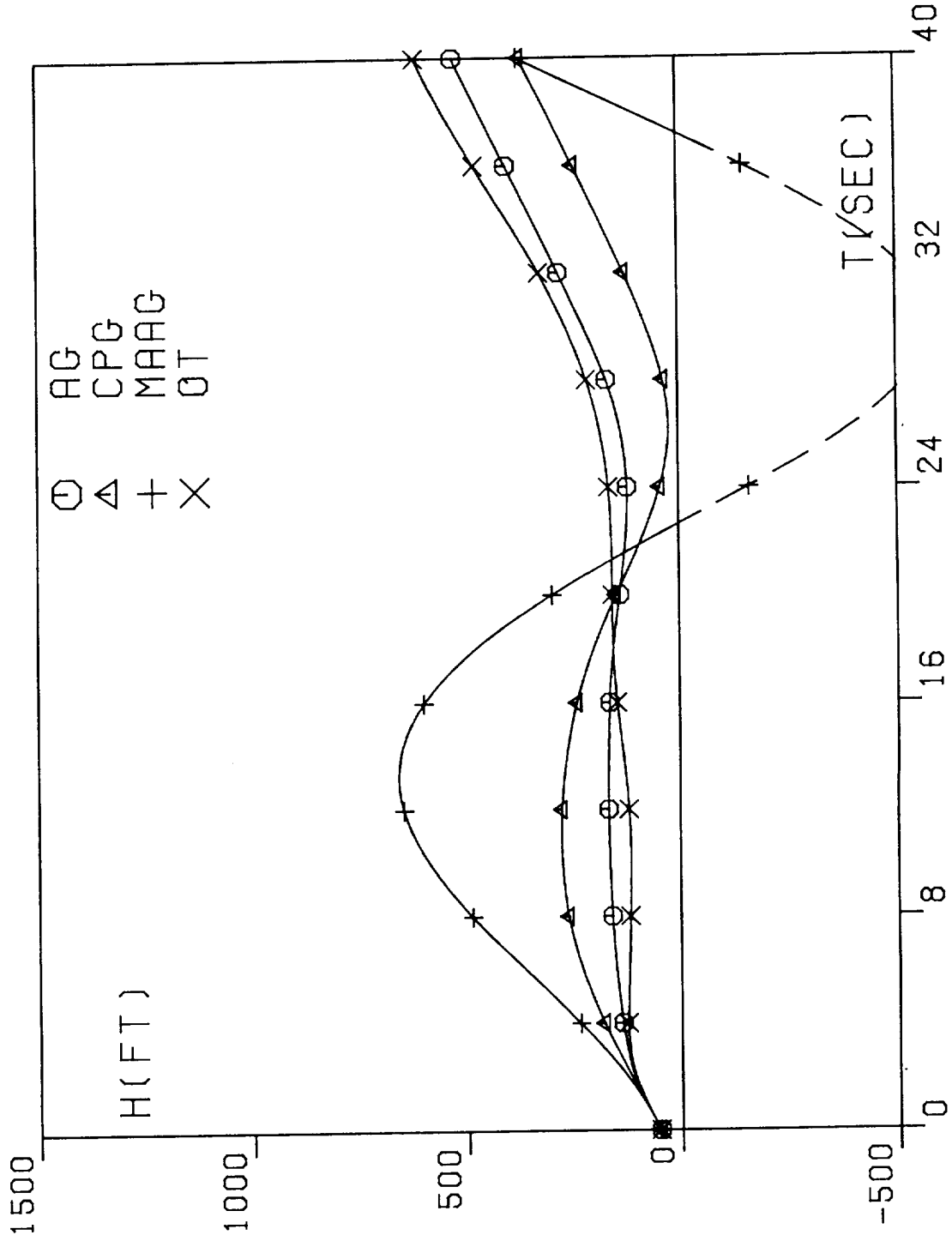


FIG. 3. GUIDANCE TRAJECTORIES,  
TAKE OFF, DWX=100FPS.

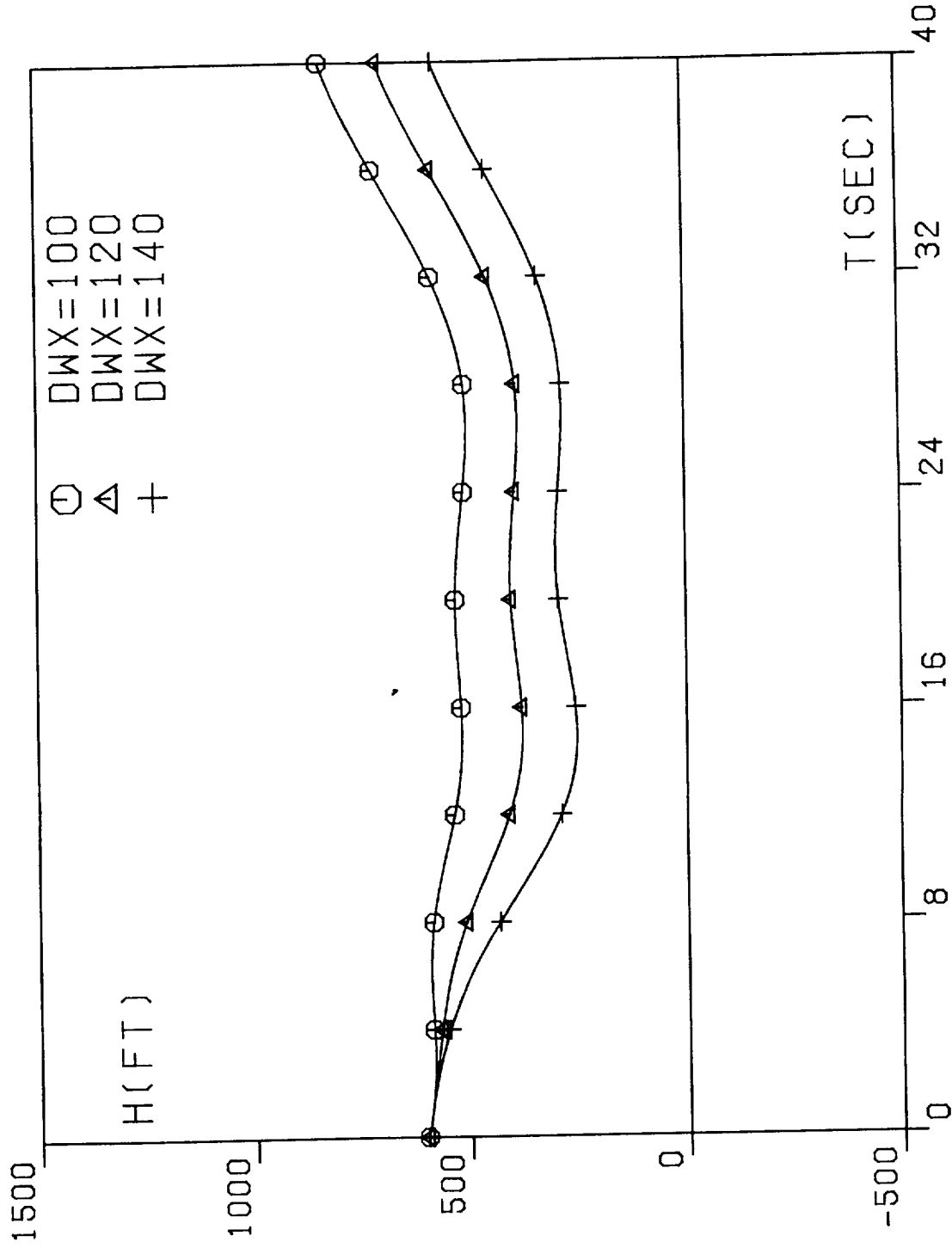


FIG. 4A. OPTIMAL TRAJECTORIES, ABORT LANDING.

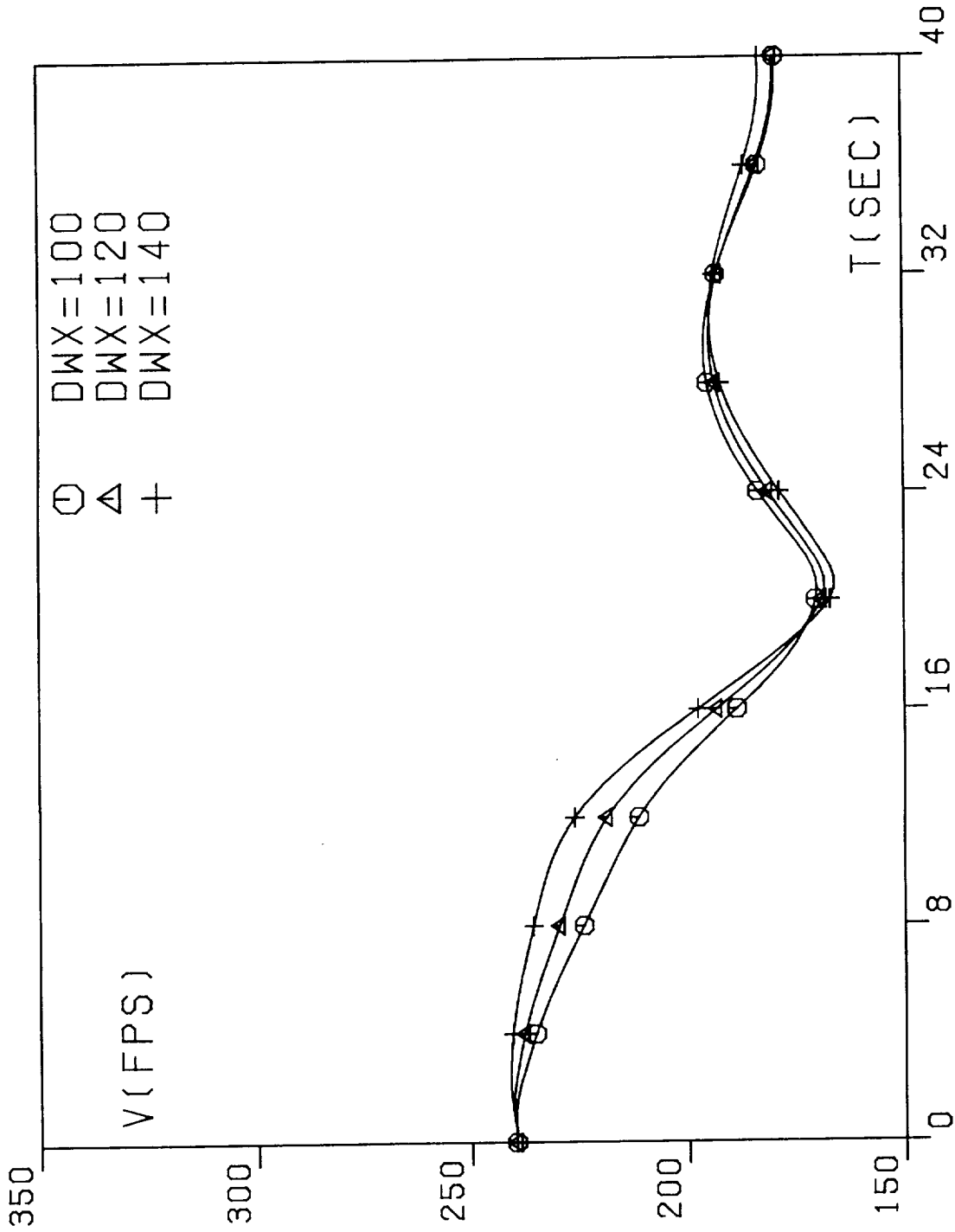


FIG. 4B. OPTIMAL TRAJECTORIES, ABORT LANDING.

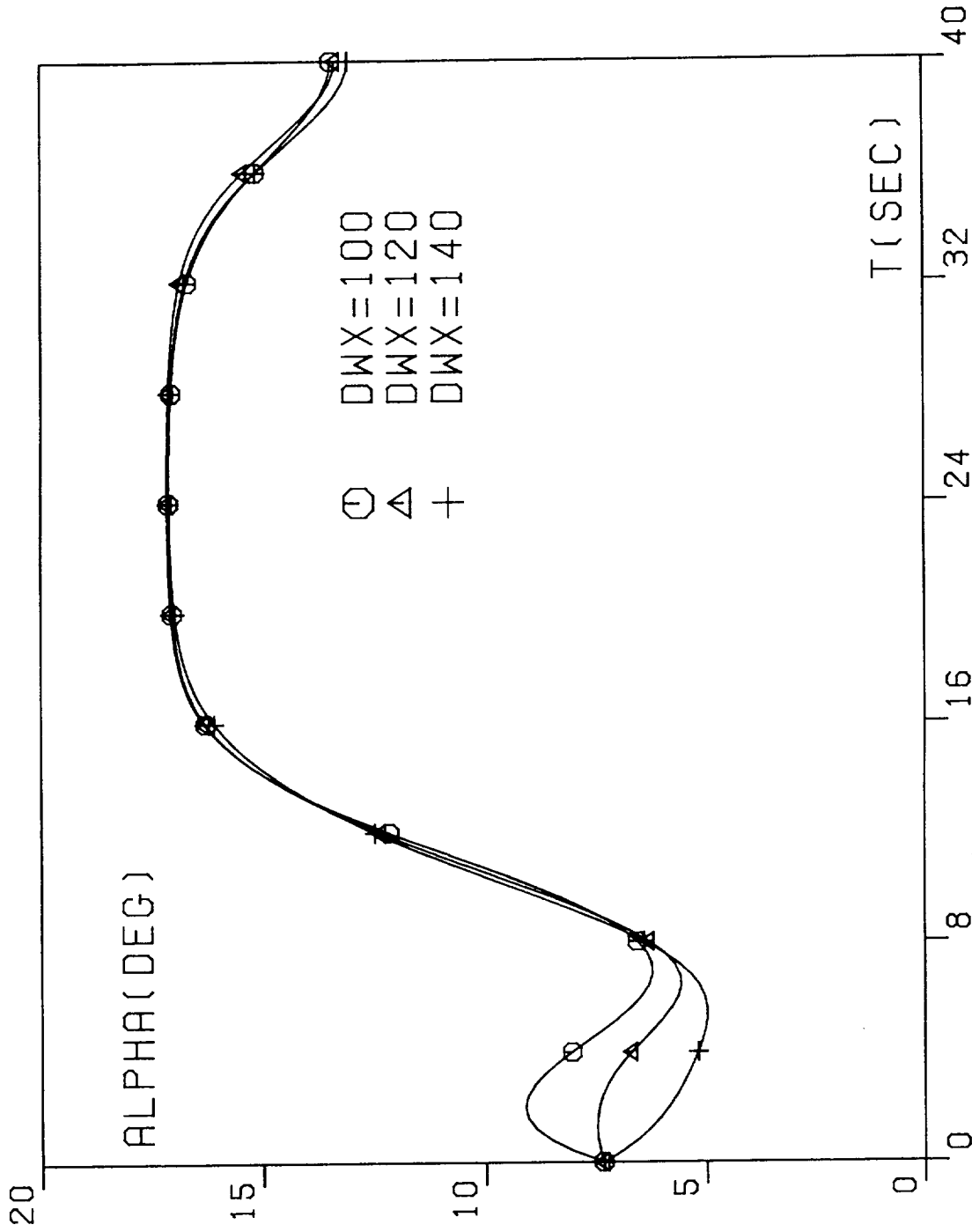


FIG. 4C. OPTIMAL TRAJECTORIES, ABORT LANDING.

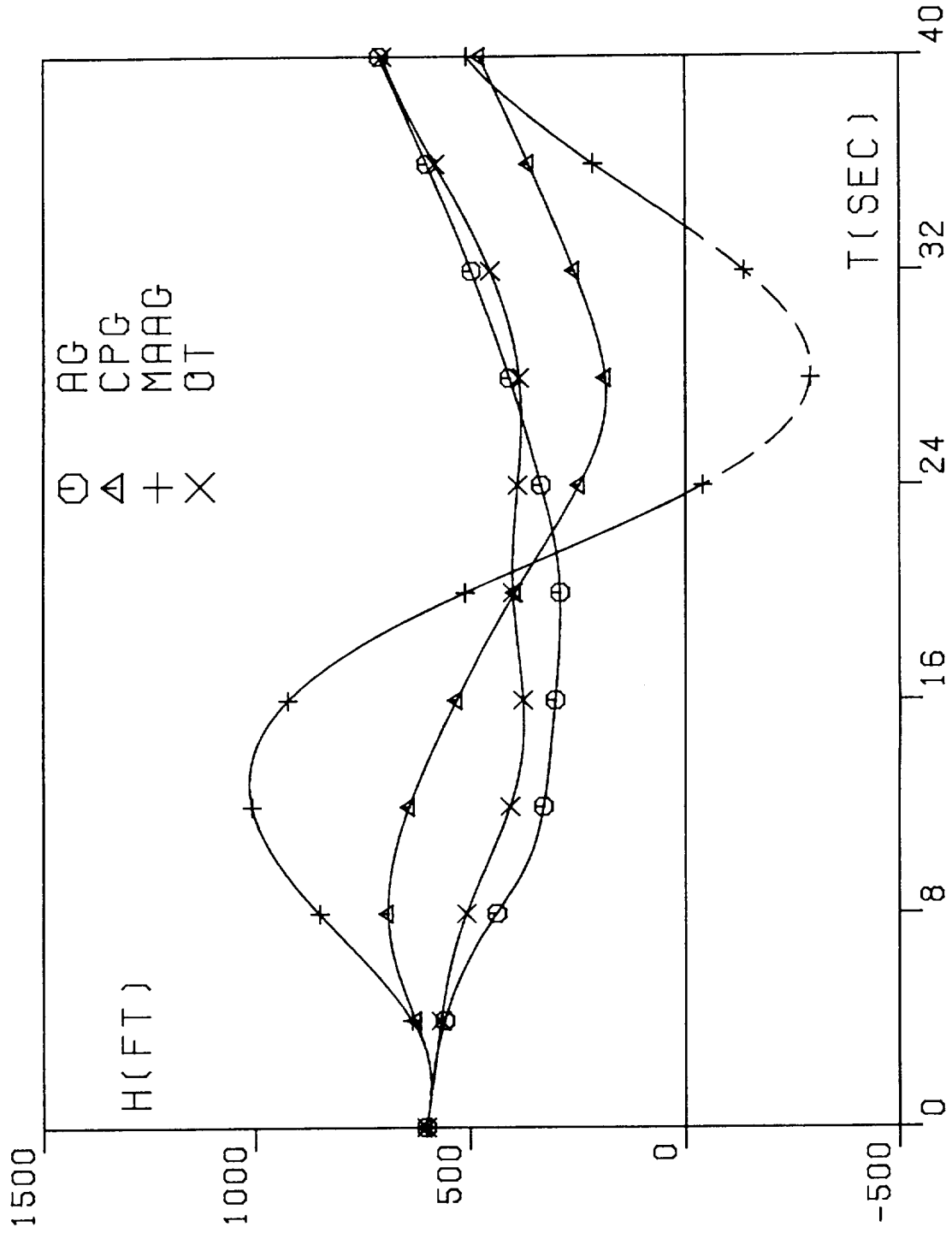


FIG. 5. GUIDANCE TRAJECTORIES, ABORT LANDING, DWX=120FPS.

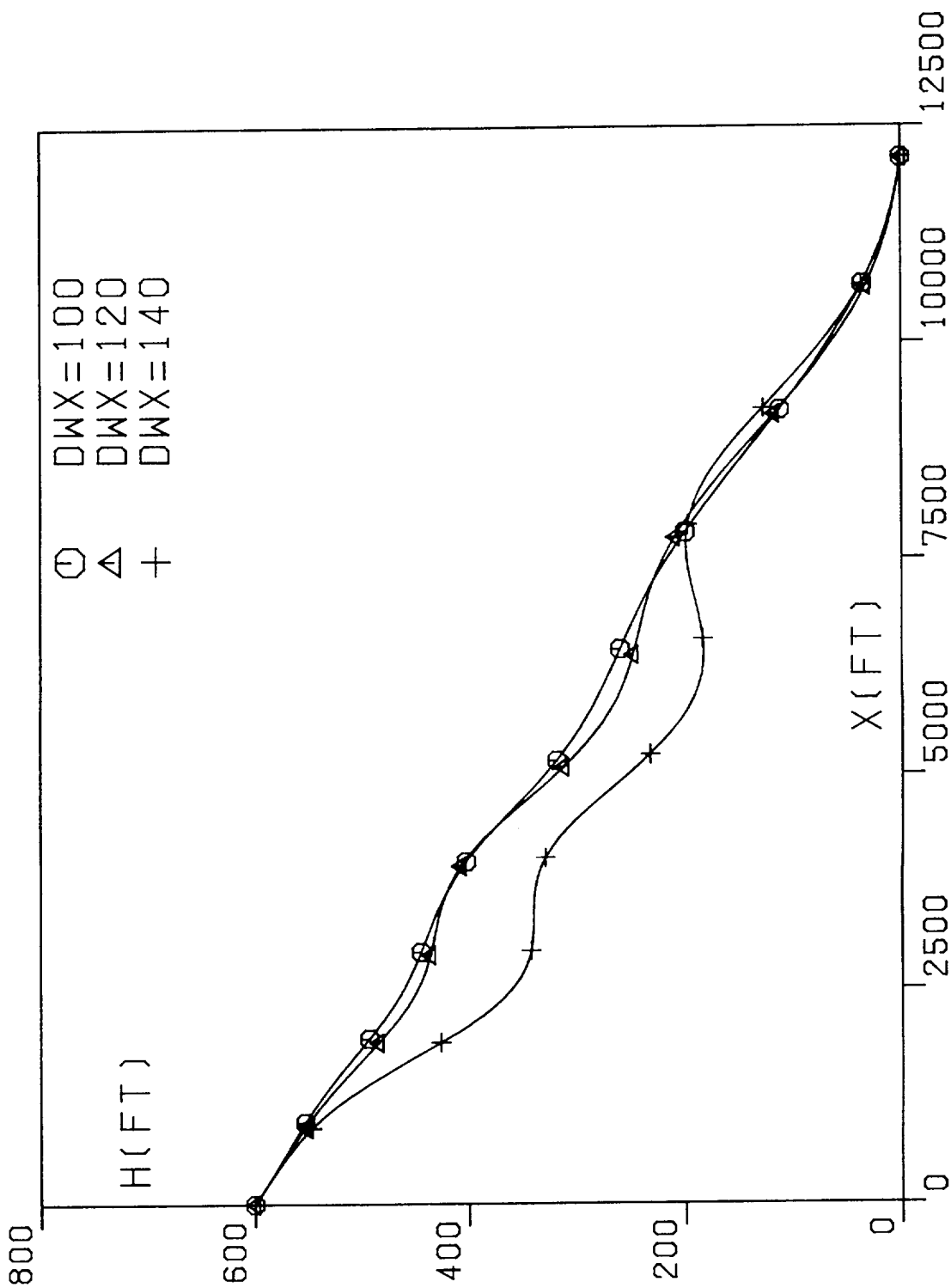


FIG. 6A. OPTIMAL TRAJECTORIES, PENETRATION LANDING.

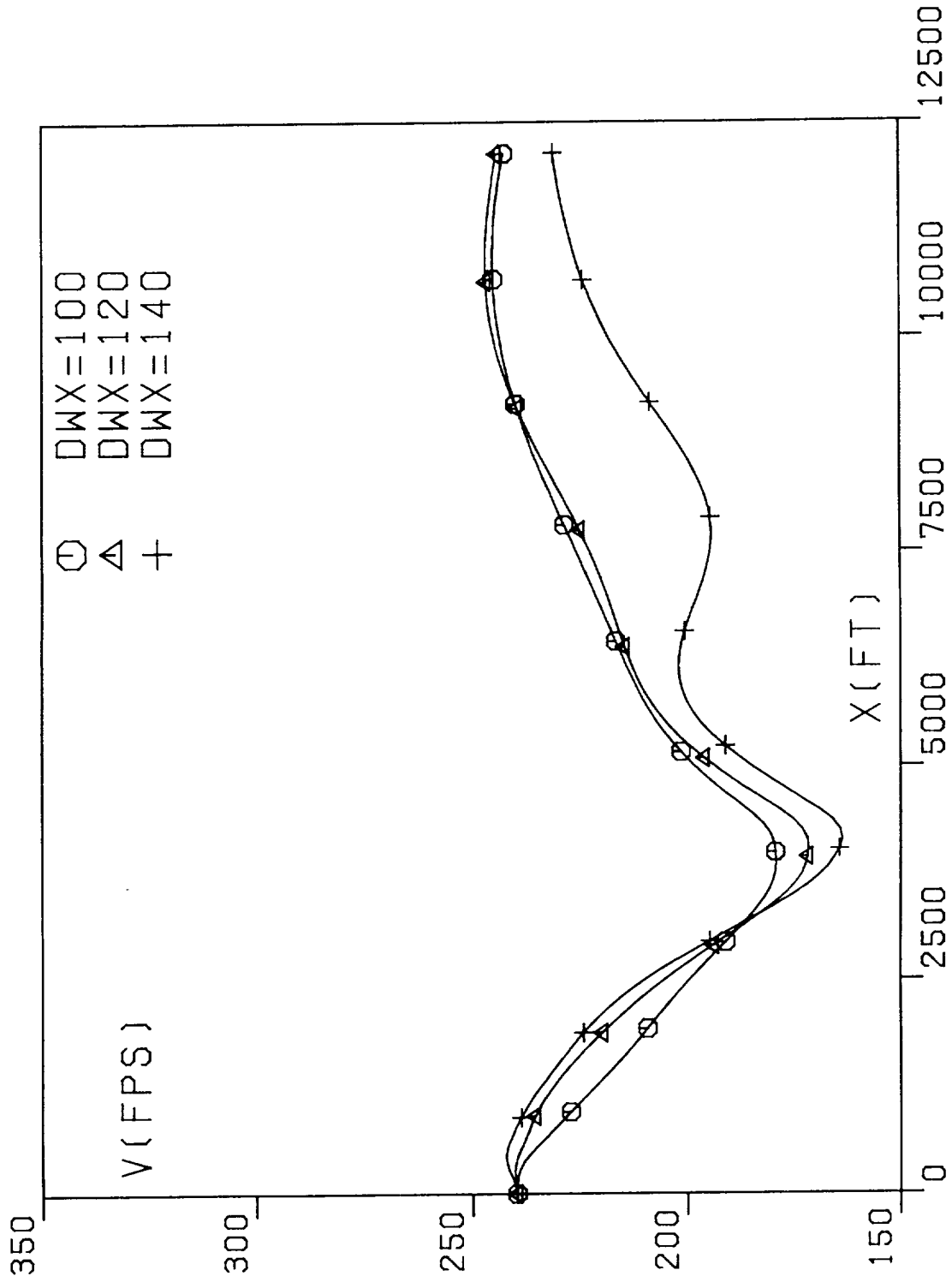


FIG. 6B. OPTIMAL TRAJECTORIES, PENETRATION LANDING.

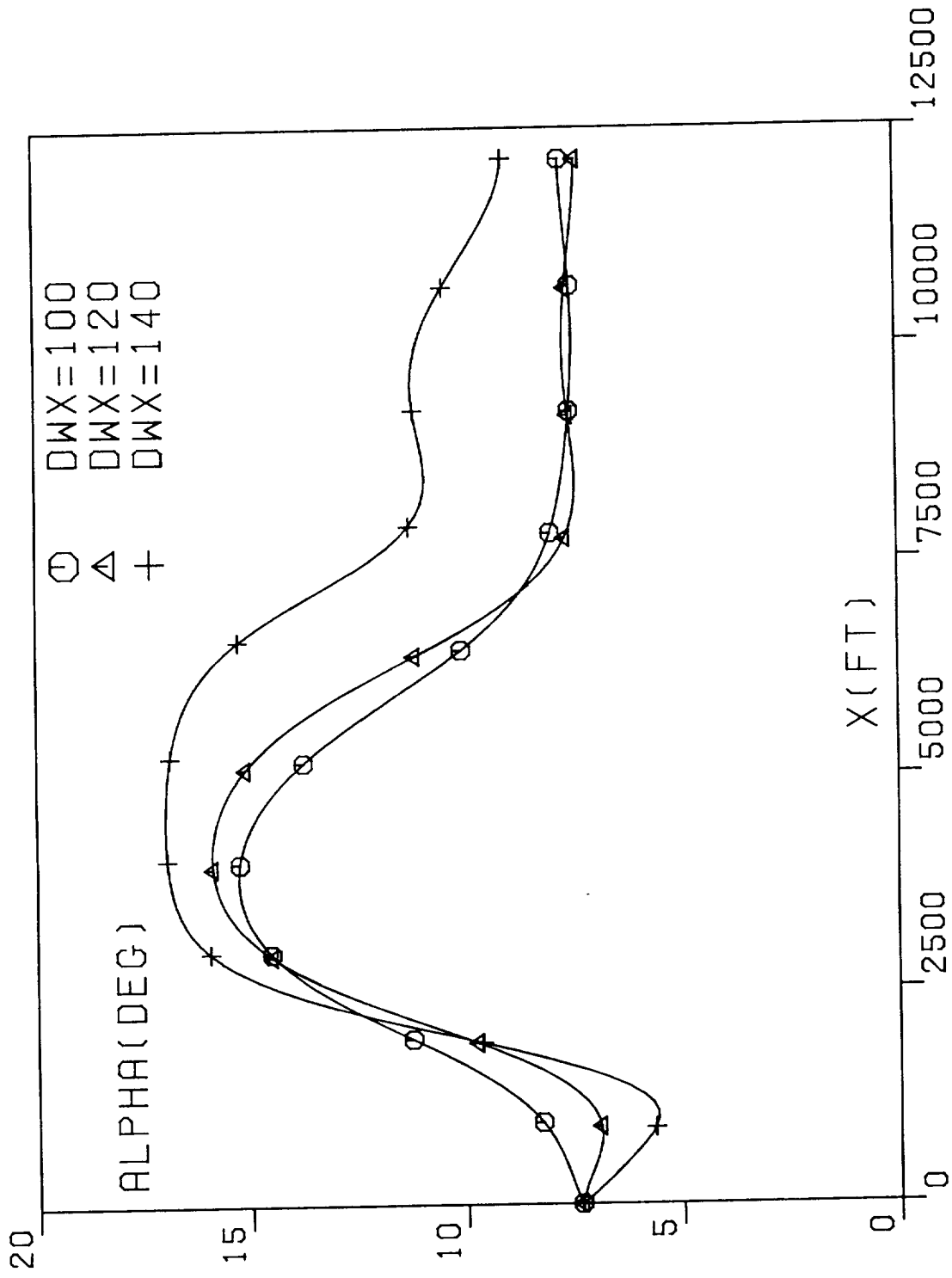


FIG. 6C. OPTIMAL TRAJECTORIES, PENETRATION LANDING.

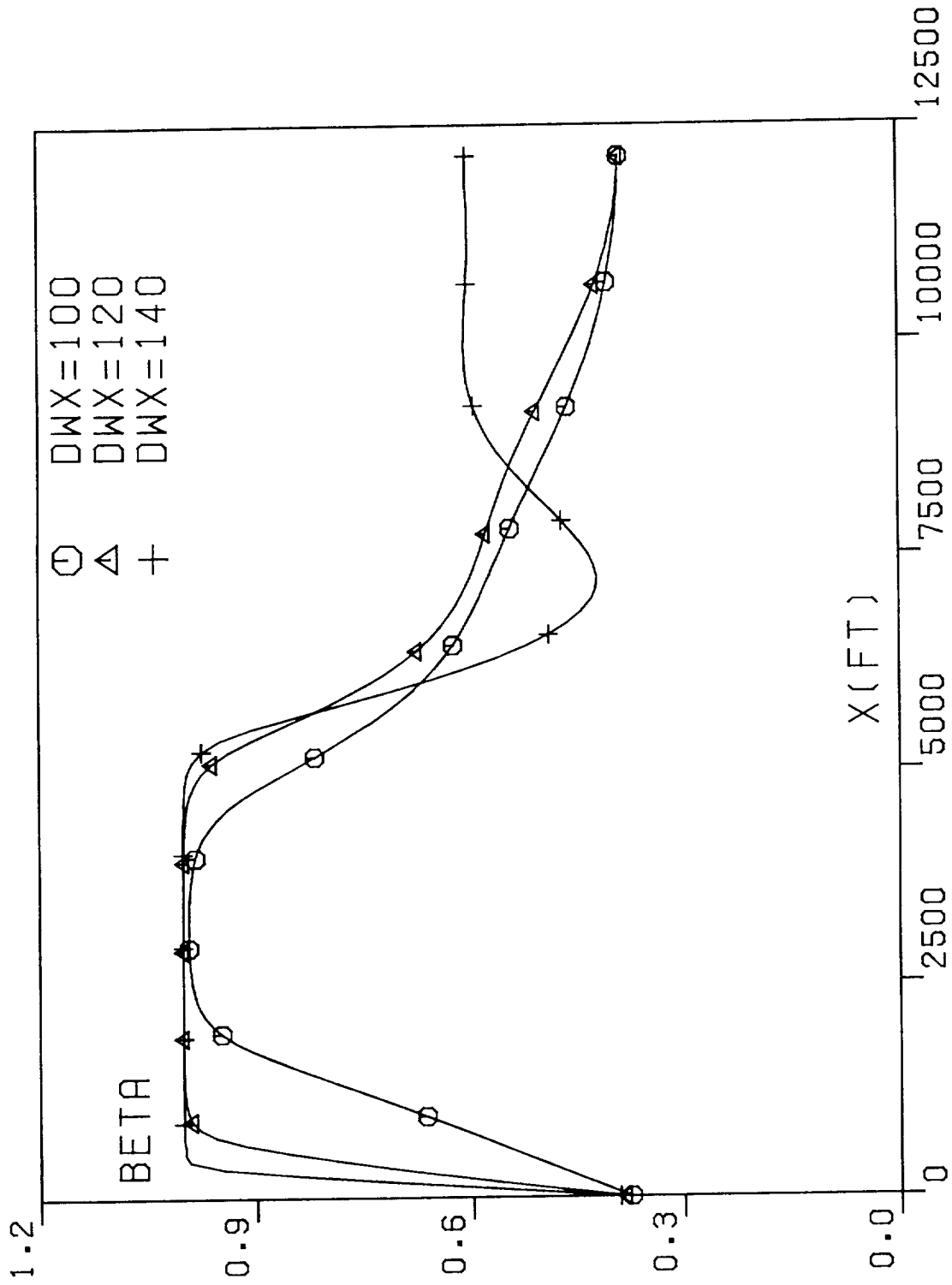


FIG. 6D. OPTIMAL TRAJECTORIES, PENETRATION LANDING.

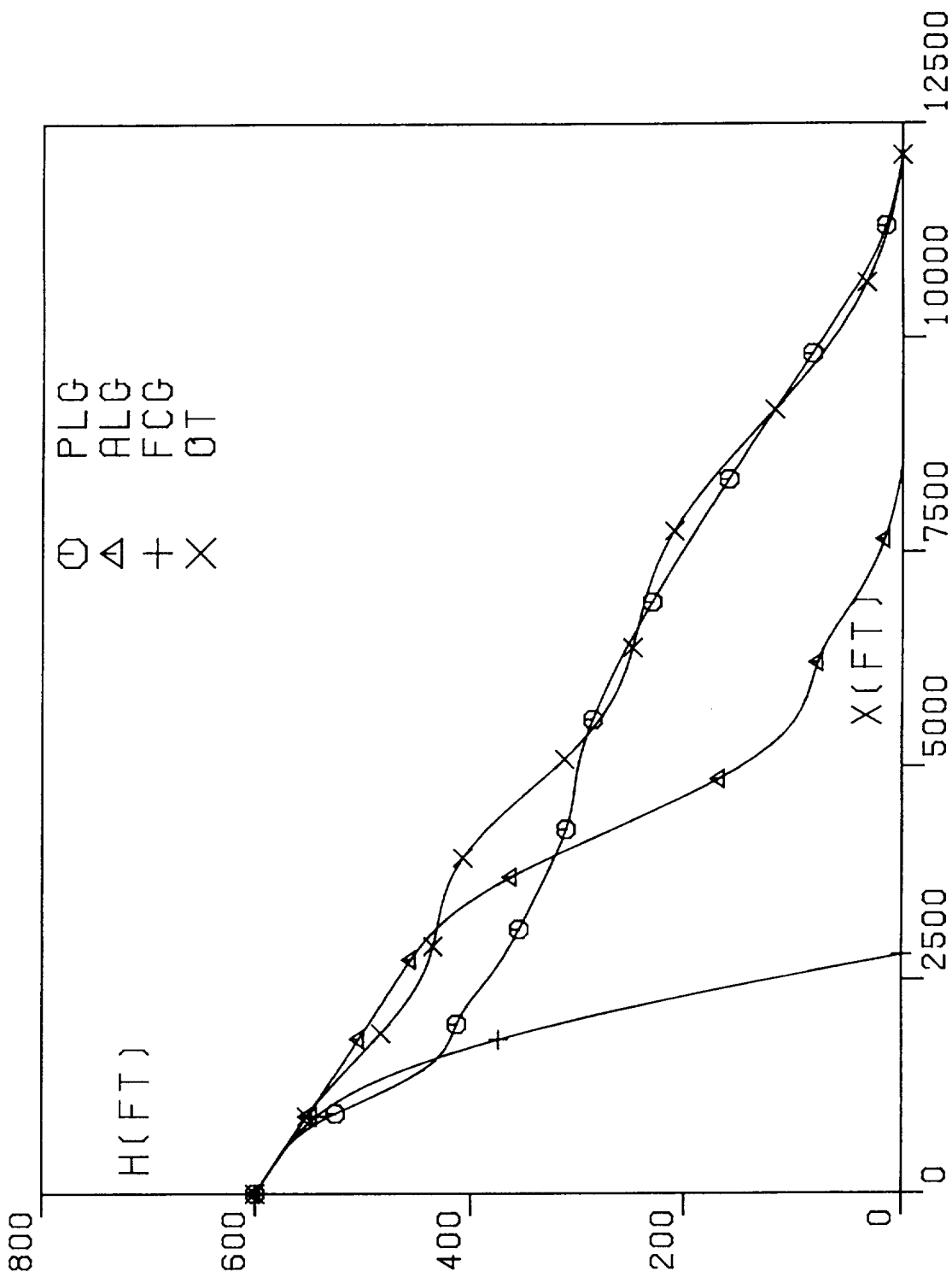


FIG. 7. GUIDANCE TRAJECTORIES, PENETRATION LANDING, DWX=120FPS.